

# Mathematical model for the in-host malaria dynamics subject to malaria vaccines

Titus Okello Orwa , Rachel Waema Mbogo  and Livingstone Serwadda Luboobi 

Institute of Mathematical Sciences, Strathmore University, Nairobi, Kenya

## ABSTRACT

Despite the success of the existing malaria control strategies, reported malaria cases are still quite high. In 2016, the WHO reported about 216 million malaria cases; 90% of which occurred in the WHO African Region. In this paper, a mathematical model for the in-host *Plasmodium falciparum* malaria subject to malaria vaccines is formulated and analysed. An efficacious pre-erythrocytic vaccine is shown to greatly reduce the severity of clinical malaria. Based on the normalized forward sensitivity index technique, the average number of merozoites released per bursting blood schizont is shown to be the most sensitive parameter in the model. Numerical simulation results further suggest that an efficacious blood stage vaccine has the potential to reduce the burst size of the blood schizonts and maximize the rate of activation of CD8+ T cells during malaria infection. Moreover, vaccine combinations that are efficacious might help in achieving a malaria free population by the year 2030. This paper provides useful insights in malaria vaccine control and a unique opportunity to intensify support and funding for malaria vaccine development.

## ARTICLE HISTORY



Received 22 June 2018  
Accepted 14 September 2018

## KEYWORDS

Malaria vaccines; vaccine efficacy; hepatocytes; CD8+ T cells; red blood cells; *Plasmodium falciparum*

## 1. Introduction

To date, the World Health Organization (WHO) considers effective vector control strategies such as long-lasting insecticidal nets (ITNs) and indoor residual spraying (IRS) as the main ways to prevent and reduce malaria transmission in communities with high malaria prevalence (Homan, 2016; WHO, 2017a). In addition, chemoprophylaxis and anti-malarial drugs such as chloroquine and artemisinin-based combination therapy (ACT) are currently used to prevent and treat clinical malaria, respectively, in different parts of the world (Bhatt et al., 2015; WHO, 2015). These strategies have contributed to the substantial global decline in malaria mortality and morbidity (Negal, Alemu, & Tasew, 2016). However, despite the success of the existing malaria prevention and control strategies, reported malaria cases are still quite high. In 2016, the WHO reported about 216 million malaria cases; 90% of which occurred in the WHO African Region (WHO, 2017b). This represented an increase of 5 million malaria cases from the year 2015.

**CONTACT** Titus Okello Orwa  [torwa@strathmore.edu](mailto:torwa@strathmore.edu)  Institute of Mathematical Sciences, Strathmore University, P.O. Box 59857-00200, Nairobi, Kenya

Malaria is a mosquito-borne infectious disease caused by an intracellular protozoan parasite of the genus *Plasmodium* (Liehl et al., 2015; Risco-Castillo et al., 2015). *Plasmodium falciparum* is the deadliest (Derbyshire, Mota, & Clardy, 2011) and predominant malaria parasite in sub-Saharan African and was responsible for 99% of all malaria cases in 2016 (WHO, 2017b). While probing for blood, female Anopheles mosquito inoculates sporozoites into the human dermis. The deposited parasites rapidly migrate to the liver, where they invade the hepatocytes with the formation of protective parasitophorous vacuole (Bertolino & Bowen, 2015; Ishino, Yano, Chinzei, & Yuda, 2004; Mota et al., 2001). During this pre-erythrocytic stage, the sporozoites undergo rapid asexual reproduction (White et al., 2014; White, 2017), develop and differentiate asymptotically into thousands of erythrocytic forms called merozoites (Sturm et al., 2006). The cyclical erythrocytic stage begins when infected hepatocytes burst open, releasing infective-merozoites into the blood stream (Halder, Murphy, Milner, & Taylor, 2007). The released merozoites quickly invade susceptible red blood cells leading to the formation of infected red blood cells (IRB) cells. The waves of bursting erythrocytes and invasions of fresh erythrocytes by secondary merozoites produce malaria characteristic symptoms such as chills and headache (Derbyshire et al., 2011). Some merozoites develop into sexual forms called gametocytes that are later sucked up by feeding mosquitoes for sexual reproduction and development within the mosquito gut (sporogonic stage). If left untreated, malaria patients may develop severe symptoms and progress to coma or death.

Parasite resistance to current antimalarial drugs (Dondorp et al., 2010; Maude et al., 2009; Sidhu, Verdier-Pinard, & Fidock, 2002; Wellem's & Plowe, 2001) and vector insecticides (Alout, Labbé, Chandre, & Cohuet, 2017a; Alout, Roche, Dabiré, & Cohuet, 2017b; Soko, Chimbari, & Mukaratirwa, 2015) poses a serious threat to malaria control. To defeat the disease, many more tools with the potential to save lives today and in the future are needed (Birkett, 2016; Greenwood & Targett, 2009; MVI, 2018). An efficacious, safe and affordable malaria vaccine would help to bridge the control gap left by other intervention measures (MVI, 2018).

A malaria vaccination strategy is performed to either induce protective immune responses prior to malaria infection or to provide protection in case of malaria attack (Arama & Troye-Blomberg, 2014). Current malaria vaccines have shown minimal efficacy (Birkett, 2016; Birkett, Moorthy, Loucq, Chitnis, & Kaslow, 2013; Miura, 2016). In the completed phase III clinical testing, RTS,S/AS01 (which is the most advanced malaria vaccine to date) showed 36.3% vaccine efficacy in children and 25.9% in infants (Birkett, 2016; Miura, 2016). Although the results of phase 3 trials are promising, a more efficacious malaria vaccine is crucial if the 2030 goal of malaria eradication by WHO is to be accomplished (malERA Consultative Group on Vaccines et al., 2011).

Although there is no licensed vaccine against malaria today, many experts believe that a malaria vaccine is a necessary tool for successful malaria elimination (MVFG, 2018; Ouattara & Laurens, 2014). There are three categories of malaria vaccine candidates: pre-erythrocytic vaccines (PEV), blood stage vaccines (BSV) and transmission blocking vaccines (TBV) that target the parasite at different stages of its life cycle (see Figure 1). PEV are designed to prevent malaria infections in humans by inducing antibodies that block invasion of hepatocytes by sporozoites and/or cell-mediated immune responses that target infected hepatocytes (Duffy, Sahu, Akue, Milman, & Anderson, 2012). In this respect, PEVs

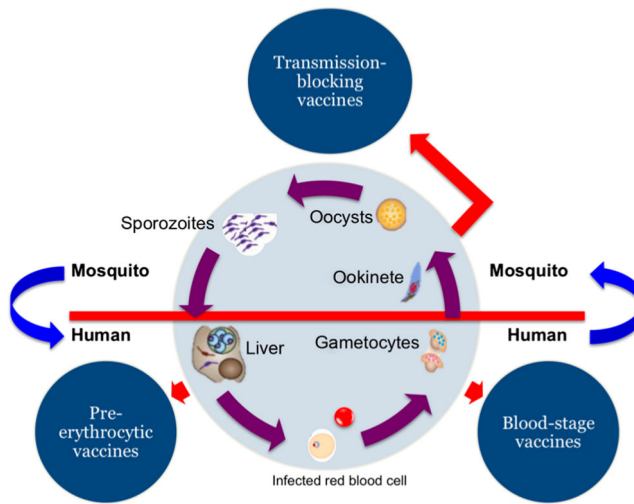


**Figure 1.** Target sites in the malaria life cycle that could be interrupted by pre-erythrocytic, blood-stage and transmission-blocking vaccines. Source: Arama and Troye-Blomberg (2014).

target malaria sporozoites thereby interrupting the life cycle of malaria parasite at an early stage (March et al., 2013). Several clinical trials (Abdulla et al., 2008; Alonso et al., 2004; Bojang et al., 2001; Polhemus et al., 2009) and (RTS, S. C. T. P., 2011) have shown the potential of RTS,S to prevent malaria infection and clinical disease in infants and young children living in sub-Saharan Africa (Birkett, 2016; Miura, 2016; RTS, S. C. T. P., 2012). PEV may also induce protection against clinical malaria at the blood stage by temporarily reducing the number of merozoites that emerge from the bursting infected liver cells (Alonso et al., 2004).

BSV on the other hand elicits anti-invasion and anti-disease responses at the blood stage (Moorthy, Good, & Hill, 2004). They, therefore, lower merozoites density and prevent clinical manifestations and hence severity of malaria infection in humans. Due to gene alteration and antigenic variation in malaria merozoites, BSV may not provide complete immunity to the host (Pandey et al., 2013). At present, merozoite surface protein 3 (MSP3) (Audran et al., 2005) and merozoite surface protein 1 (MSP1) (Ogutu et al., 2009) are the leading blood stage vaccine candidates for *Plasmodium falciparum* (Plowe, Alonso, & Hoffman, 2009).

The aim of TBV is to stop subsequent generation of infectious malaria sporozoites from the female anopheles mosquito vector. TBV induces antibodies against antigens on gametes, zygote and ookinetes, blocking ookinete to oocyst transition and hence stopping parasite development within the mosquito midgut (Carter, Mendis, Miller, Molineaux, & Saul, 2000). Consequently, the density of malaria sporozoites in the mosquito salivary glands is decreased. The leading malaria vaccine candidate in this category is the *Plasmodium falciparum* ookinete surface antigens (Pfs25) (Arevalo-Herrera et al., 2005; Hisaeda et al., 2000).

Due to intracellular infections, *P. falciparum* parasites are susceptible to immune-mediated control by CD8<sup>+</sup> T cells, which target intracellular pathogens (Villarino, 2013). The CD8<sup>+</sup> T cells have both direct and indirect effector pathways for parasite elimination

at the liver stage. The indirect mechanism includes the production of IFN- $\gamma$  and TNF, whereas the direct mechanism involves the release of perforin and granzymes (Nganou-Makamdop, van Gemert, Arens, Hermsen, & Sauerwein, 2012). IFN- $\gamma$  suppresses parasite development through direct impairment of parasite differentiation in hepatocytes (Mellouk et al., 1987). Moreover, IFN- $\gamma$  increases the expression of nitric oxide synthase which leads to subsequent increase in nitric oxide that confers protection against *P. falciparum* (Seguin et al., 1994). Although CD8+ T cells are sufficiently primed during blood stage malaria, they offer very minimal contribution to protective immunity. It is thought in Villarino (2013) that vascular endothelial cells that acquire antigen from IRBCs stimulate CD8+ T cells to release perforin and granzyme B during blood stage malaria. The capacity of CD8+ T cells to eradicate malaria parasites and infected cells both at the liver stage and at the blood stage is therefore considered in this paper.

A lot of research has been carried on clinical malaria control (Austin, White, & Anderson, 1998; Hellriegel, 1992; Kamangira, Nyamugure, & Magombedze, 2014; Li, Ruan, & Xiao, 2011; Tumwiine, Hove-Musekwa, & Nyabadza, 2014). Some of these models have focussed on the role of the host's immune cells (Malaguarnera & Musumeci, 2002; Tumwiine et al., 2014) while others are based on the use of antimalarial drugs (Kamangira et al., 2014; Magombedze, Chiyaka, & Mukandavire, 2011) in controlling clinical malaria. In Chiyaka, Garira, and Dube (2008), both the immune cells and malaria chemotherapy controls are considered. In Rouzine and McKenzie (2003), the role of innate immunity in mediating synchronization between the replication cycles of parasites in different erythrocytes is explored. Kamangira et al. (2014) investigated erythrocytes–malaria parasite dynamics in the presence of immune response and/or drug intervention at the erythrocytic stage. Results in Nannyonga, Mwanga, Haario, Mbalawata, and Heilio (2014) showed that malaria merozoites can be absorbed in already IRB cells, leading to faster rapture of IRB cells and hence causing anaemia. Tabo, Luboobi, and Ssebuliba (2017) incorporated the liver stage in their model and investigated treatment as a control strategy for blood stage malaria. Results from their study showed that a treatment strategy using highly effective drugs targeting specific parameters can reduce malaria progression and control the disease in humans. The above research activities have been very insightful in understanding in-host malaria dynamics and control, however, none of these investigations has attempted to evaluate the possible impacts of malaria vaccines in controlling clinical *P. falciparum* malaria both at the liver stage and at the blood stage. In this study, we formulate a more detailed in-host malaria model that considers parasite–cell interactions at the liver stage and the blood stage subject to malaria vaccines. Our goals are to study the interacting cell-parasite populations through a mathematical model and to numerically investigate the possible impacts of malaria vaccines on the severity of *P. falciparum* malaria infection.

The rest of the paper is organized as follows. In the following section, we incorporate vaccination control to a formulated in-host malaria model and describe the corresponding model parameters and variables. The vaccine model is analysed and its vaccine reproductive number together with parameter sensitivity analysis is computed in Section 3. In Section 4, we investigate the effects of malaria vaccines and vaccine efficacy on malaria dynamics and malaria severity. A discussion and conclusion complete the paper in Sections 5 and 6, respectively.

## 2. Model formulation

We present a mathematical model of in-host *P. falciparum* malaria dynamics in the presence of malaria vaccines. The compartmental model is an extension of the hepatocytic–erythrocytic in-host malaria model in Orwa, Mbogo, and Luboobi (2018) in which two compartments of gametocytes  $G(t)$  and CD8+ T cells  $W(t)$  are added to capture the effects of the transmission blocking vaccines and the general effects of CD8+ T cells on the density of the IRB cells and hence malaria infection dynamics. The rest of the populations include susceptible liver hepatocytes  $H(t)$ , infected liver hepatocytes  $X(t)$ , malaria sporozoites  $S(t)$ , susceptible red blood cells  $R(t)$ , infected red blood cells (blood trophozoites)  $T(t)$ , infected red blood cells (blood schizonts)  $C(t)$  and malaria merozoites  $M(t)$ .

During feeding, infected mosquito injects  $\Lambda$  sporozoites into the human skin. These sporozoites traverse Kupffer and endothelial cells and enter the liver hepatocytes. Susceptible liver hepatocytes are recruited by self-replication at a rate  $\lambda_h$ . Following invasion by sporozoites at the rate  $\beta_s$ , infected hepatocytes  $X$  progress to hepatic-schizont which eventual burst open at the rate  $\mu_x$  to release merozoites into the blood stream. The initial recruitment of the merozoites is hence represented by the term  $N\mu_x X$ , where  $N$  is the number of merozoites released per bursting infected hepatocyte. The released merozoites invade and infect the host's red blood cells at a rate  $\beta_r$  and die naturally at the rate  $\mu_m$ .

Based on their stage of infection, we classify IRB cells as either blood trophozoites (early stage of infection) or blood schizonts (late stage of infection). Susceptible RBCs are recruited at a constant rate  $\lambda_r$  from the bone marrow and their concentration decreases through natural death at the rate  $\mu_r$  or due to invasion by the merozoites at the rate  $\beta_r$ . Following merozoite invasion, susceptible RBCs move to the class of infected red blood cells (blood trophozoites)  $T$ . The generated blood trophozoites decay naturally at a rate  $\mu_t$  or progress into blood schizonts  $C$  class at the rate  $\gamma$ . Mature blood schizonts burst open to release more merozoites into blood stream. This is represented by the term  $(P\mu_c C/1 + dW)$ , where  $P$  denotes the number of merozoites released per bursting blood schizont and  $\mu_c$  is the decay rate of the blood schizonts.

At the pre-erythrocytic stage, the malaria sporozoites are debilitated by vaccine-induced anti-CSP antibodies (PEV) as they molt through the tissues (Mellouk et al., 1990; Schwenk et al., 2003). This reduced invasion of hepatocytes by the malaria sporozoites is represented by the term  $\beta_s(1 - \nu)SH$ , where  $0 < \nu < 1$  is the efficacy of the pre-erythrocytic vaccine. Sporozoites that successfully invade the hepatocytes are, however, targeted by vaccine-induced CSP-specific CD8+ T cells (PEV). The CD8+ T cells kill the resulting infected hepatocyte (Renia et al., 1991; Sun et al., 2003; White et al., 2013). The killing of infected hepatocytes reduces the burst size  $N$  of the infected hepatocytes. This is represented by the term  $(1 - b)N$ , where  $0 < b < 1$  is the probability with which the vaccine inhibits merozoite emergence from infected hepatocyte.

An unbounded bilinear function  $rEI$  is considered in Anderson, May, and Gupta (1989), Niger and Gumel (2011) and Hetzel and Anderson (1996) to model the killing of infected cells  $I$  by the CD8+ T cells  $E$ . The simple mass-action term depends solely on the product of the concentration of the immune cells and the density of the infected cells. However, if we take into account the fact that cell proliferation can saturate then the nonlinear bounded

Michaelis–Menten–Monod function, presented in Equation (1) is most reasonable (Agur, Abiri, & Van der Ploeg, 1989; Antia, Levin, & May, 1994).

$$\nabla = \nabla_{\max} \frac{B}{K_b + B}, \quad (1)$$

where  $B$  is the concentration of substrate,  $\nabla$  is the growth rate of the microorganisms  $B$ ,  $\nabla_{\max}$  is the maximum specific growth rate of  $B$  and  $K_b$  is the half-velocity constant,  $\nabla/\nabla_{\max}$ .

In Pilyugin and Antia (2000), the nonlinear bounded Michaelis–Menten–Monod function (1) is used to model the handling time in immune response and their targets and how it affects the infection. In this paper, we adopt such a nonlinear bounded function ( $p_1IE/(1 + \beta I)$ ) in Chiyaka et al. (2008), where it is used to describe the killing of infected erythrocytes  $I$  by the immune cells  $E$  (CD8+ T cells, in our case). This formulation has also been used in Cai, Tuncer, and Martcheva (2017) and Selemeni, Luboobi, and Nkansah-Gyekye (2017). The parameter  $p_1$  describes the rate of removal of  $I$  by  $E$  and  $1/\beta$  is the saturation constant that stimulates the proliferation of the CD8+ T cells to grow at half their maximum rate.

The effects of the BSV on merozoite invasion of the red blood cells are represented by the term  $((1 - \varrho)\beta_r RM)/(1 + dW)$ , where  $0 < \varrho < 1$  is the efficacy of the BSV and  $1/d$  is a saturation constant that stimulates CD8+ T cells to grow at half their maximum rate. In addition, BSV reduces the density of merozoites that are released per bursting blood schizont, so that the burst size  $P$  becomes  $(1 - a)P$ , where  $0 < a < 1$  accounts for the vaccine-induced reduction of merozoites released per bursting IRB cell. BSV is further assumed to enhance the production of CD8+ T cells at a rate  $\tau$ , where  $\tau > 1$ . For purposes of simulation, we assume  $1 < \tau < 2$ . Administered TBV is assumed to reduce the recruitment rate of the sporozoites  $\Lambda$  to  $(1 - \chi)\Lambda$ , where  $0 < \chi < 1$  is the efficacy of the TBV. Moreover, the inoculated sporozoites are assumed to die naturally at the rate  $\mu_s$ .

The immune cells (CD8+ T cells) are recruitment at a constant rate  $\lambda_w$  from the thymus. Furthermore, the presence of infected cells such as infected hepatocytes, blood trophozoites and blood schizonts stimulates the production of CD8+ T cells. The increased production of  $W(t)$  due to  $X(t)$ ,  $T(t)$  and  $C(t)$  is also modelled using the nonlinear bounded Michaelis–Menten–Monod function (1) and is represented by the terms  $(\delta_x WX/1 + \varepsilon_0 X)$ ,  $(\delta_t WT/1 + \varepsilon_1 T)$  and  $(\delta_c WC/1 + \varepsilon_2 C)$ , respectively. The parameter  $\delta_i | i = \{x, t, c\}$  represents the immunogenicity of infected hepatocytes, blood trophozoites and blood schizonts respectively. On the other hand, the phagocytotic effects of CD8+ T cells on infected cells ( $X$ ,  $T$  and  $C$ ) are represented by the terms  $(k_x(1 - \nu)WX/1 + \varepsilon_0 X)$ ,  $(k_t(1 - \varrho)WT/1 + \varepsilon_1 T)$  and  $(k_c(1 - \varrho)WC/1 + \varepsilon_2 C)$ , where  $k_j | j = \{x, t, c\}$  is the immunosensitivity of  $X, T$  and  $C$ , respectively.

The density of blood schizonts  $C$  decreases when they burst open to release merozoites into blood stream or when they die naturally at the rate  $\mu_c$ . A proportion  $\pi$  of the released merozoites develops into gametocytes  $G(t)$  whose natural decay rate is denoted by  $\mu_g$ . Just like the susceptible hepatocytes whose natural mortality is at the rate  $\mu_h$ , we assume a constant decay rates  $\mu_t$  and  $\mu_w$  for blood trophozoites and the CD8+ T cells respectively.

The descriptions of the variables and parameters used in the model are summarized in Tables 1 and 2 respectively.

**Table 1.** Description of variables.

Variable	Description
$H(t)$	Concentration of uninfected hepatocytes
$X(t)$	Concentration of infected hepatocytes
$R(t)$	Concentration of susceptible red blood cells
$T(t)$	Concentration of blood trophozoites
$C(t)$	Concentration of blood schizonts
$S(t)$	Concentration of sporozoites
$M(t)$	Concentration of merozoites in blood
$G(t)$	Concentration of gametocytes in blood
$W(t)$	Concentration of CD8+ T cells

**Table 2.** Description of parameters.

Parameter	Description
$\Delta$	The rate of injection of sporozoites into liver due to mosquito bites
$\mu_s$	The decay rate of sporozoites
$\lambda_h$	Rate of production of susceptible hepatocytes from the bone marrow
$\lambda_r$	Rate of production of susceptible RBC by the bone marrow
$\mu_h, \mu_x$	Death rate of susceptible hepatocyte and infected hepatocyte respectively
$\pi$	Proportion of parasites that become gametocytes per dying blood schizont
$k_x, k_t, k_c$	Immunosensitivity of infected hepatocytes, blood trophozoites and blood schizonts respectively
$\delta_x, \delta_t, \delta_c$	Immunogenicity of infected hepatocytes, blood trophozoites and blood schizonts respectively
$\beta_s$	Infection rate of hepatocytes by sporozoites
$\mu_r$	The natural mortality rate of RBC
$\beta_r$	Rate of infection of RBCs by merozoites
$\mu_t, \mu_c$	The rate of decay of blood trophozoites and blood schizonts respectively
$\mu_m, \mu_g$	Decay rate of merozoites and gametocytes respectively
$\gamma$	Progression rate of IRB cells from trophozoite to schizont stage
$\chi$	Efficacy of transmission blocking vaccine
$\varrho$	Efficacy of blood stage vaccine.
$d$	The rate of inhibition of immune response
$\lambda_w$	The rate of production of CD8+ T cells
$1/\varepsilon_0, 1/\varepsilon_1, 1/\varepsilon_2$	half saturation constants for infected hepatocytes, blood trophozoites and blood schizonts respectively
$\tau$	A parameter that accounts for vaccine-induced enhanced production of CD8+ T cells
$\nu$	Efficacy of pre-erythrocytic stage vaccine
$\mu_w$	Decay rate of CD8+ T cells
$b$	A parameter that accounts for PEV-induced reduction of merozoites released per bursting infected hepatocyte
$a$	A parameter that accounts for BSV-induced reduction of merozoites released per bursting blood schizont
$P$	The average number of merozoites released per bursting blood schizont
$N$	The average number of merozoites released per bursting infected hepatocytes

The in-host malaria dynamics subject to vaccination is represented in the compartmental flow diagram in Figure 2. Based on the above model description and assumptions, the in-host malaria model that takes vaccines into account is formulated using a system of

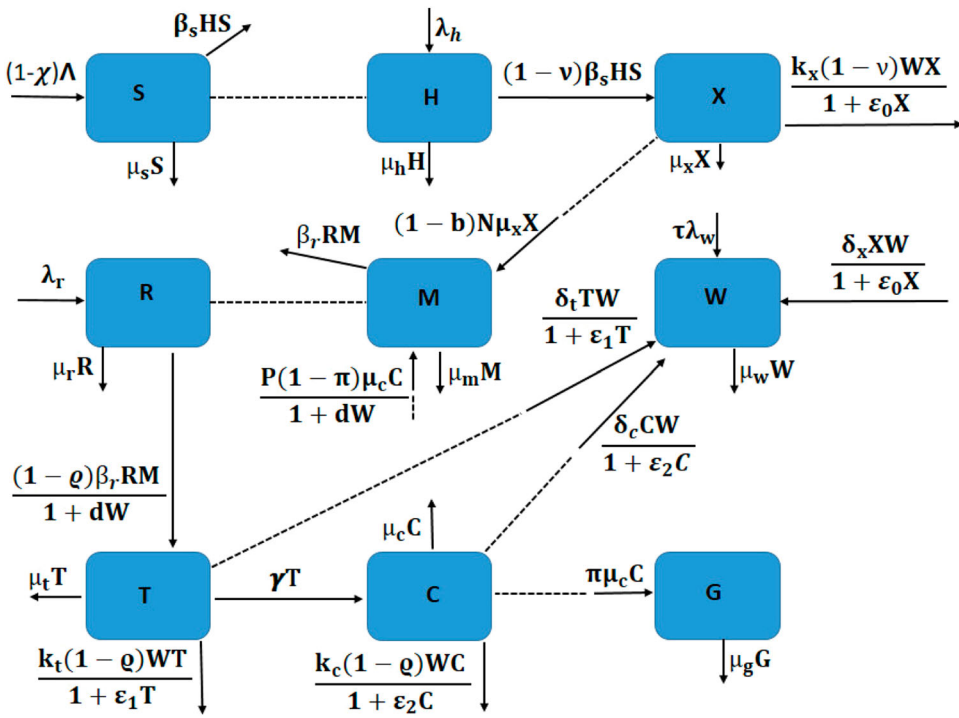


**Figure 2.** Schematic diagram for in-host malaria with vaccine therapy. The dotted lines without arrows indicate cell–parasite interaction and the solid lines show progression from one compartment to another.

nonlinear ordinary differential equations and presented as follows:

$$\left. \begin{aligned}
 \frac{dS}{dt} &= (1 - \chi)\Lambda - \mu_s S - \beta_s HS, \\
 \frac{dH}{dt} &= \lambda_h - \mu_h H - \beta_s(1 - v)HS, \\
 \frac{dX}{dt} &= \beta_s(1 - v)SH - \mu_x X - \frac{k_x(1 - v)WX}{1 + \varepsilon_0 X}, \\
 \frac{dR}{dt} &= \lambda_r - \frac{(1 - \varrho)\beta_r RM}{1 + dW} - \mu_r R, \\
 \frac{dT}{dt} &= \frac{(1 - \varrho)\beta_r RM}{1 + dW} - \mu_t T - \gamma T - \frac{k_t(1 - \varrho)WT}{1 + \varepsilon_1 T}, \\
 \frac{dC}{dt} &= \gamma T - \mu_c C - \frac{k_c(1 - \varrho)WC}{1 + \varepsilon_2 C}, \\
 \frac{dM}{dt} &= (1 - b)N\mu_x X + \frac{P(1 - \pi)(1 - a)\mu_c C}{1 + dW} - \mu_m M - \beta_r RM, \\
 \frac{dG}{dt} &= \pi\mu_c C - \mu_g G, \\
 \frac{dW}{dt} &= \tau\lambda_w + W \left( \frac{\delta_x X}{1 + \varepsilon_0 X} + \frac{\delta_t T}{1 + \varepsilon_1 T} + \frac{\delta_c C}{1 + \varepsilon_2 C} \right) - \mu_w W.
 \end{aligned} \right\} \quad (2)$$



We assume that all the parameters used in the model are positive and the initial conditions for system (2) are:  $H(0) \geq 0, X(0) \geq 0, S(0) \geq 0, R(0) \geq 0, T(0) \geq 0, C(0) \geq 0, M(0) \geq 0, G(0) \geq 0, W(0) \geq 0$ .

### 3. Model analysis

#### 3.1. Well-posedness of the model

We aim to evaluate the effects of the different vaccines on the concentration of infected hepatocytes and infected red blood cells. Therefore, the model should be biologically coherent. That is, all the state variables and their solutions must be non-negative and bounded, respectively, in the region  $\Phi$ , where

$$\begin{aligned} \Phi &= \left\{ (H, X, R, T, C, S, M, G, W) \in \mathbb{R}_+^9 : N_r(t) \leq \max \left\{ N_r(0), \frac{\lambda_r}{\mu_1} \right\}, \right. \\ N_h(t) &\leq \max \left\{ N_h(0), \frac{\lambda_h}{\mu_2} \right\}, N_p(t) \leq \max \left\{ N_p(0), \frac{(1 - \chi)\Lambda}{\mu_3} \right\}, \\ W(t) &\leq \max \left\{ W(0), \frac{\tau\lambda_w}{\mu_w} \right\} \left. \right\}, \end{aligned} \tag{3}$$

and  $N_r(t) = R(t) + T(t) + C(t)$ ,  $N_h(t) = H(t) + X(t)$ ,  $N_p(t) = S(t) + M(t) + G(t)$ ,  $\mu_1 = \min\{\mu_r, \mu_t, \mu_c\}$ ,  $\mu_2 = \min\{\mu_h, \mu_x\}$  and  $\mu_3 = \min\{\mu_s, \mu_m, \mu_g\}$ .

For the in-host malaria model (2) to be biologically meaningful, we prove the following theorem.

**Theorem 3.1:** *The region  $\Phi$  is positively invariant with respect to the in-host malaria model (2), and a non-negative solution  $(H(t), X(t), R(t), T(t), C(t), S(t), M(t), G(t), W(t))$  exists  $\forall t \geq 0$ .*

**Proof:** From the sporozoite compartment  $S(t)$  in system (2), we have

$$\frac{dS}{dt} = (1 - \chi)\Lambda - \mu_s S - \beta_s HS \geq -(\mu_s + \beta_s H)S. \tag{4}$$

Integrating (4) yields

$$S(t) \geq S(0) \exp\left\{-\left(\mu_s t + \beta_s \int_0^t H(n)dn\right)\right\}. \tag{5}$$

This shows that in the absence of malaria interventions,  $S(t) \geq 0$  for all time  $t \geq 0$ .

Using the same argument above, it is easy to see that

$$H(t) \geq H(0) \exp\left\{-\left(\mu_h t + \beta_s(1 - v) \int_0^t S(n)dn\right)\right\}. \tag{6}$$

This process can be repeated for all the state variables so that  $S(t), H(t), X(t), R(t), T(t), C(t), M(t), G(t), W(t)$  are all positive for all  $t \geq 0$ . Thus the solutions of in-host malaria model (2) remain positive in  $\Phi$  for all time  $t \geq 0$ . A quick guide on proof for positivity and

boundedness is available in Nyabadza, Njagarah, and Smith (2013) and Traoré, Sangaré, and Traoré (2017).

To show that the solutions of model system (2) are bounded, we let  $N_r$  be the total concentration of the red blood cells in the human host, that is  $N_r(t) = R(t) + T(t) + C(t)$  and

$$\frac{dN_r}{dt} = \lambda_r - \mu_r R - \mu_t T - \mu_c C - \left( \frac{k_t(1-\varrho)WT}{1+\varepsilon_1 T} + \frac{k_c(1-\varrho)WC}{1+\varepsilon_2 C} \right), \quad (7)$$

$$\leq \lambda_r - \mu_1 N_r \quad \text{where} \quad \mu_1 = \min\{\mu_r, \mu_t, \mu_c\}. \quad (8)$$

Using the initial condition  $N_r(0) = N_{r0} > 0$ , Equation (8) is solved by integration into

$$N_r(t) \leq \frac{\lambda_r}{\mu_1} + e^{-\mu_1 t} \left( N_r(0) - \frac{\lambda_r}{\mu_1} \right).$$

This implies that at any time  $t$ ,  $N_r(t) \leq \max\{N_r(0), \frac{\lambda_r}{\mu_1}\}$ . This approach can similarly be applied to the population of hepatocytes  $N_h = H(t) + X(t)$ , population of parasites  $N_p = S(t) + M(t) + G(t)$  and to the concentration of CD8+ T cells  $W(t)$ , so that we obtain

$$\begin{aligned} N_h(t) &\leq \max \left\{ N_h(0), \frac{\lambda_h}{\mu_2} \right\}, \quad \text{where } \mu_2 = \min\{\mu_h, \mu_x\}; \\ N_p(t) &\leq \max \left\{ N_p(0), \frac{(1-\chi)\Lambda}{\mu_3} \right\}, \quad \text{where } \mu_3 = \min\{\mu_s, \mu_m, \mu_g\} \quad \text{and} \\ W(t) &\leq \max \left\{ W(0), \frac{\tau\lambda_w}{\mu_w} \right\}. \end{aligned}$$

The above analysis shows that the region  $\Phi$  is positively invariant and attracting for system (2) and the model is hence well posed for study. ■

### 3.2. Parasite free equilibrium and vaccination reproduction number

The parasite free equilibrium (PFE),  $E_v$ , depicts the absence of malaria parasites from the human host. The PFE of the in-host malaria model system (2) exists and is given by

$$E_v = (H^0, X^0, R^0, T^0, C^0, S^0, M^0, G^0, W^0) = \left( \frac{\lambda_h}{\mu_h}, 0, \frac{\lambda_r}{\mu_r}, 0, 0, 0, 0, 0, \frac{\tau\lambda_w}{\mu_w} \right). \quad (9)$$

The vaccination reproduction number (denoted by  $R_v$ ), on the other hand, is a threshold quantity which governs the spread of the infection. It represents on average the number of new infected cells (RBCs or liver hepatocytes) generated by a single infectious merozoite (or sporozoites) at the blood (or liver) stage in the presence of malaria vaccines. Using the next generation matrix approach (Diekmann, Heesterbeek, & Metz, 1990; Van den Driessche & Watmough, 2002), the matrix  $\mathcal{F}_1$  that represents the rate of appearance of new infections and the matrix  $\mathcal{V}_1$  that denotes the transfer of infections from one compartment

to the other are respectively given as

$$\mathcal{F}_1 = \begin{pmatrix} \beta_s(1 - v)SH \\ 0 \\ \frac{(1 - \varrho)\beta_rRM}{1 + dW} \\ 0 \\ 0 \\ 0 \end{pmatrix} \text{ and}$$

$$\mathcal{V}_1 = \begin{pmatrix} \mu_x X + \frac{k_x(1 - v)WX}{1 + \varepsilon_0 X} \\ -(1 - \chi)\Lambda + \mu_s S + \beta_s SH \\ \mu_t T + \gamma T + \frac{k_t(1 - \varrho)WT}{1 + \varepsilon_1 T} \\ -\gamma T + \mu_c C + \frac{k_c(1 - \varrho)WC}{1 + \varepsilon_2 C} \\ -(1 - b)N\mu_x X - \frac{P(1 - \pi)(1 - a)\mu_c C}{1 + dW} + \mu_m M + \beta_r RM \\ -\pi\mu_c C + \mu_g G \end{pmatrix}. \tag{10}$$

Upon taking the partial derivatives of the terms in  $\mathcal{F}_1$  and  $\mathcal{V}_1$  and evaluating at the parasite free equilibrium  $E_v$ , we obtain a non-negative matrix  $F_1$  and a non-singular matrix  $V_1$  as follows.

$$F_1 = \begin{pmatrix} 0 & \frac{(1 - v)\beta_s\lambda_h}{\mu_h} & 0 & 0 & 0 & 0 \\ 0 & 0 & 0 & 0 & 0 & 0 \\ 0 & 0 & 0 & 0 & \frac{(1 - e)\beta_r\lambda_r\mu_w}{\mu_r(d\tau\lambda_w + \mu_w)} & 0 \\ 0 & 0 & 0 & 0 & 0 & 0 \\ 0 & 0 & 0 & 0 & 0 & 0 \\ 0 & 0 & 0 & 0 & 0 & 0 \end{pmatrix} \tag{11}$$

and

$$V_1 = \begin{pmatrix} V_a & 0 & 0 & 0 & 0 & 0 \\ 0 & \frac{\beta_s\lambda_h}{\mu_h} + \mu_s & 0 & 0 & 0 & 0 \\ 0 & 0 & V_b & 0 & 0 & 0 \\ 0 & 0 & -\gamma & \frac{(1 - \varrho)\tau k_c\lambda_w}{\mu_w} + \mu_c & 0 & 0 \\ -(1 - b)N\mu_x & 0 & 0 & -\frac{(1 - a)P(1 - \pi)\mu_c}{d\tau\lambda_w + 1} & \frac{\beta_r\lambda_r}{\mu_r} + \mu_m & 0 \\ 0 & 0 & 0 & -\pi\mu_c & 0 & \mu_g \end{pmatrix}, \tag{12}$$

where  $V_a = (((1 - \varrho)\tau k_x\lambda_w)/\mu_w) + \mu_x$  and  $V_b = \gamma + \mu_t + (((1 - \varrho)\tau k_t\lambda_w)/\mu_w)$ .

The vaccination reproduction number is the spectral radius of  $(F_1 V_1^{-1})$ . That is,

$$R_v = \frac{P(1-\pi)(1-a)(1-\varrho)\gamma\beta_r\lambda_r\mu_c}{\mu_r \left(\frac{d\tau\lambda_w + \mu_w}{\mu_w}\right)^2 \left(\mu_m + \frac{\beta_r\lambda_r}{\mu_r}\right) \left(\frac{(1-\varrho)\tau k_c\lambda_w}{\mu_w} + \mu_c\right) \left(\frac{(1-\varrho)\tau k_t\lambda_w}{\mu_w} + \gamma + \mu_t\right)}. \quad (13)$$

In the absence of malaria vaccines ( $\chi = \varrho = v = a = b = 0, \tau = 1$ ), model (2) has a basic reproduction number  $R_m$  given by

$$R_m = \frac{P(1-\pi)\gamma\beta_r\lambda_r\mu_c}{\mu_r \left(\frac{d\lambda_w + \mu_w}{\mu_w}\right)^2 \left(\frac{k_c\lambda_w}{\mu_w} + \mu_c\right) \left(\mu_m + \frac{\beta_r\lambda_r}{\mu_r}\right) \left(\gamma + \frac{k_t\lambda_w}{\mu_w} + \mu_t\right)}. \quad (14)$$

On comparing Equations (13) and (14), we deduce the following:

$$R_m = R_v \times \Theta^{**}, \quad (15)$$

where

$$\Theta^{**} = \frac{(1-a)(1-e) \left(\frac{d\lambda_w}{\mu_w} + 1\right) (d\lambda_w + \mu_w) \left(\frac{k_c\lambda_w}{\mu_w} + \mu_c\right) \left(\gamma + \frac{k_t\lambda_w}{\mu_w} + \mu_t\right)}{\mu_w \left(\frac{d\tau\lambda_w}{\mu_w} + 1\right)^2 \left(\frac{(1-e)\tau k_c\lambda_w}{\mu_w} + \mu_c\right) \left(\gamma + \frac{(1-e)\tau k_t\lambda_w}{\mu_w} + \mu_t\right)}.$$

We observe from Equation (15) that in the absence of vaccination,  $R_v = R_m$ . However, the introduction of malaria vaccines reduces the basic reproduction number by a factor of  $0 < \Theta^{**} < 1$ . The use of efficacious malaria vaccines therefore has a great potential in reducing mortality due to *P. falciparum* malaria disease.

### 3.3. Sensitivity analysis

The main concern in the control of infectious diseases is the capacity of the infection to invade the population. The threshold quantity called the vaccine reproduction number provides a reasonable measure of the ability of the infective malaria parasites to invade the susceptible cell populations (Heesterbeek & Dietz, 1996). When  $R_v < 1$ , the infective parasites produce less than one new infection per infection period and the disease subsequently dies out. However, when  $R_v > 1$ , an infective parasite generates several infections leading to disease severity. In light of this, we carry out sensitivity analysis of model  $R_v$  in (13) so as to determine important parameters in the dynamics of *P. falciparum* malaria in the presence of vaccine controls. Following Arriola and Hyman (2007), the normalized forward sensitivity indices of  $R_v$  with respect to input parameters  $a$ , denoted by  $\Gamma_a$ , is given by

$$\Gamma_a = \frac{\partial R_v}{\partial a} \times \frac{a}{R_v}. \quad (16)$$

Based on the model  $R_v$  and the parameter values in Table 4, we derive the following analytical expressions for sensitivity indices of  $R_v$  with respect to parameters  $\varrho, P, \pi$  and  $\tau$ . A part from the parameter  $P$ , whose sensitivity index does not depend on other parameter values, the rest of the expressions for the sensitivity indices are complex (see for instance

(18)–(20)). We therefore evaluate the sensitivity indices of  $R_v$  using the baseline parameter values in Table 4.

$$\Gamma_P = +1 \tag{17}$$

$$\Gamma_\rho = \rho \left( \tau \lambda_w \left( -\frac{k_c}{(\rho - 1)\tau k_c \lambda_w - \mu_c \mu_w} - \frac{k_t}{(\rho - 1)\tau k_t \lambda_w - \mu_w (\gamma + \mu_t)} \right) + \frac{1}{\rho - 1} \right) \tag{18}$$

$$\Gamma_\pi = -\frac{\Lambda}{1 - \Lambda} \tag{19}$$

$$\Gamma_\tau = \tau \lambda_w \left( -\frac{(\rho - 1)k_c}{(\rho - 1)\tau k_c \lambda_w - \mu_c \mu_w} - \frac{2d}{d\tau \lambda_w + \mu_w} - \frac{(\rho - 1)k_t}{(\rho - 1)\tau k_t \lambda_w - \mu_w (\gamma + \mu_t)} \right). \tag{20}$$

Using Mathematica software, the sensitivity results for the 17 parameters in  $R_v$  are as shown in Table 3. The rate of merozoite invasion  $\beta_r$ , the rate of progression of infected red blood cells from the trophozoite state to blood schizonts  $\gamma$  and the average number of merozoites released per bursting blood schizont  $P$  increase (or decrease) the vaccine reproduction number when they are increased (or decreased) as shown in Table 3. Malaria vaccine development should target these parameters to reduce malaria disease progression in humans. On the other hand, the higher the efficacy of blood stage vaccine  $\rho$ , the lower the value of  $R_v$ . A highly efficient erythrocytic vaccine has the potential to eradicate clinical malaria. The proportions of merozoites that development into gametocytes  $\pi$  is also shown to decrease the value of  $R_v$  when they are increased. The higher the concentration of gametocytes, the lower the density of merozoites in the host’s blood. Although this would minimize secondary and subsequent erythrocytic invasions and hence malaria severity, it has the potential to enhance parasite transmission to the mosquito vector. This is due to increased concentration of gametocytes per blood sample per mosquito bite.

The density of merozoites released per bursting infected red blood cells and the efficacy of the blood stage vaccine are shown to be the most sensitive parameters in influencing in-host malaria progression. For example, a 10% increase (or decrease) on  $P$  will cause a 10% increase (or decrease) in  $R_v$ . These two parameters should hence be carefully estimated (Mikucki, 2012) and clinical malaria control using antimalarial drugs and malaria vaccines should target the two parameters. This is because a small variation in such a parameter will lead to large quantitative changes in  $R_v$  and hence on malaria disease progression.

**Table 3.** The sensitivity indices of  $R_v$  with respect model parameters.

Parameter	Sensitivity index	Parameter	Sensitivity index
P	+1	$\pi$	-0.25
$a$	-0.25	$\rho$	-0.770486
$\gamma$	+0.293702	$\beta_r$	+0.0000663956
$\lambda_r$	+0.0000664	$\mu_c$	+0.0000247494
$\mu_r$	-0.000066396	$d$	-0.0222497
$\tau$	-0.080544	$\lambda_w$	-0.080544
$\mu_w$	+0.080	$\mu_m$	-0.00006639
$k_c$	-0.0000247494	$k_t$	-0.0582696
$\mu_t$	-0.235433		

### 3.4. Local stability of parasite free equilibrium

The local stability of  $E_v$  is investigated as follows. We begin by linearizing model system (2) around  $E_v$  so that we have the following Jacobian matrix  $J_1$ .

$$J_1 = \begin{pmatrix} -\mu_h & 0 & -A_0 & 0 & 0 & 0 & 0 & 0 & 0 \\ 0 & -A_1 & A_2 & 0 & 0 & 0 & 0 & 0 & 0 \\ 0 & 0 & -A_3 & 0 & 0 & 0 & 0 & 0 & 0 \\ 0 & 0 & 0 & -\mu_r & 0 & 0 & -A_4 & 0 & 0 \\ 0 & 0 & 0 & 0 & -A_5 & 0 & A_6 & 0 & 0 \\ 0 & 0 & 0 & 0 & \gamma & -A_7 & 0 & 0 & 0 \\ 0 & A_{11} & 0 & 0 & 0 & A_8 & -A_9 & 0 & 0 \\ 0 & 0 & 0 & 0 & 0 & \pi\mu_t & 0 & -\mu_g & 0 \\ 0 & \frac{\tau\delta_x\lambda_w}{\mu_w} & 0 & 0 & A_{10} & \frac{\tau\delta_c\lambda_w}{\mu_w} & 0 & 0 & -\mu_w \end{pmatrix} \quad (21)$$

where

$$\begin{aligned} A_0 &= \frac{(1-v)\beta_s\lambda_h}{\mu_h}, A_1 = \frac{(1-v)\tau k_x\lambda_w}{\mu_w} + \mu_x, A_2 = \frac{(1-v)\beta_s\lambda_h}{\mu_h}, \\ A_3 &= \frac{\beta_s\lambda_h}{\mu_h} + \mu_s, A_4 = \frac{(1-\varrho)\beta_r\lambda_h}{\mu_h(\frac{d\tau\lambda_w}{\mu_w} + 1)}, A_5 = \gamma + \mu_t + \frac{(1-\varrho)\tau k_t\lambda_w}{\mu_w}, \\ A_6 &= \frac{(1-\varrho)\beta_r\lambda_h}{\mu_h(\frac{d\tau\lambda_w}{\mu_w} + 1)}, A_7 = \frac{(1-\varrho)\tau k_c\lambda_w}{\mu_w} + \mu_c, A_8 = \frac{(1-a)P(1-\pi)\mu_c}{\frac{d\tau\lambda_w}{\mu_w} + 1}, \\ A_9 &= \frac{\beta_r\lambda_h}{\mu_h} + \mu_m, A_{10} = \frac{\tau\delta_t\lambda_w}{\mu_w} \quad \text{and} \quad A_{11} = (1-b)N\mu_x. \end{aligned}$$

It is easy to see from matrix  $J_1$  that the first eigenvalue,  $\lambda_1 = -\mu_h < 0$ . Upon deleting row 1 and column 1 from which  $\lambda_1$  is placed, a new sub-matrix  $J_2$  is produced.

$$J_2 = \begin{pmatrix} -A_1 & A_2 & 0 & 0 & 0 & 0 & 0 & 0 \\ 0 & -A_3 & 0 & 0 & 0 & 0 & 0 & 0 \\ 0 & 0 & -\mu_r & 0 & 0 & A_4 & 0 & 0 \\ 0 & 0 & 0 & -A_5 & 0 & A_6 & 0 & 0 \\ 0 & 0 & 0 & \gamma & -A_7 & 0 & 0 & 0 \\ A_{11} & 0 & 0 & 0 & A_8 & -A_9 & 0 & 0 \\ 0 & 0 & 0 & 0 & \pi\mu_t & 0 & -\mu_g & 0 \\ \frac{\tau\delta_x\lambda_w}{\mu_w} & 0 & 0 & A_{10} & \frac{\tau\delta_c\lambda_w}{\mu_w} & 0 & 0 & -\mu_w \end{pmatrix}. \quad (22)$$

On applying the above procedure to columns 3, 7 and 8 and their corresponding rows in matrix (22), we obtain the next three eigenvalues:  $\lambda_2 = -\mu_r < 0$ ,  $\lambda_3 = -\mu_g < 0$  and  $\lambda_4 = -\mu_w < 0$ . The resultant matrix  $J_3$  is as follows:

$$J_3 = \begin{pmatrix} -A_1 & A_2 & 0 & 0 & 0 \\ 0 & -A_3 & 0 & 0 & 0 \\ 0 & 0 & -A_5 & 0 & A_6 \\ 0 & 0 & \gamma & -A_7 & 0 \\ A_{11} & 0 & 0 & A_8 & -A_9 \end{pmatrix}. \quad (23)$$

The rest of the eigenvalues are obtained by solving the characteristic equation of matrix  $J_3$ :

$$\lambda^5 + \beta_1\lambda^4 + \beta_2\lambda^3 + \beta_3\lambda^2 + \beta_4\lambda + \beta_5 = 0, \tag{24}$$

where

$$\beta_1 = A_1 + A_3 + A_5 + A_7 + A_9 > 0, \tag{25}$$

$$\begin{aligned} \beta_2 = & A_1A_3 + A_1A_5 + A_3A_5 + A_1A_7 + A_3A_7 + A_5A_7 \\ & + A_1A_9 + A_3A_9 + A_5A_9 + A_7A_9 > 0, \end{aligned} \tag{26}$$

$$\beta_3 = A_1A_3A_5 + A_1A_3A_7 + A_1A_5A_7 + A_3A_5A_7 + A_1A_3A_9 + A_1A_5A_9 + A_3A_5A_9 \tag{27}$$

$$+ A_1A_7A_9 + A_3A_7A_9 + A_5A_8A_9 \left[ (1 - R_v) \left( \frac{A_6^2 A_7 A_8}{\lambda_r} \right) \right], \tag{28}$$

$$\beta_4 = A_6A_8(A_1A_8)[(1 - R_v)] + A_1A_3A_5A_7 + A_1A_3A_5A_9 + A_1A_3A_7A_9 + A_1A_5A_7A_9 \tag{29}$$

$$\beta_5 = A_1A_3A_5A_7A_9 \left[ (1 - R_v) \frac{A_6}{\lambda_r} \right]. \tag{30}$$

Equation (24) has negative roots (eigenvalues) if all its coefficients terms are positive. That is,  $\beta_1 > 0$ ,  $\beta_2 > 0$ ,  $\beta_3 > 0$ ,  $\beta_4 > 0$  and  $\beta_5 > 0$ . We can clearly see from Equations (25) and (26) that  $\beta_1$  and  $\beta_2$  are positive terms. However, the coefficients  $\beta_3$ ,  $\beta_4$  and  $\beta_5$  can only be positive if the vaccine reproduction number  $R_v$  is less than unity,  $R_v < 1$ .

Thus, using Theorem 2 in Van den Driessche and Watmough (2002), the following lemma is established.

**Lemma 3.1:** *The disease free equilibrium  $E_v$  is locally asymptotically stable if  $R_v < 1$  and unstable if  $R_v > 1$ .*

Lemma 3.1 shows that if we are to eliminate the malaria parasite following malaria infection, then we have to administer a vaccine or combinations of vaccines that would guarantee the existence of a stable disease free equilibrium. Epidemiologically, when  $R_v < 1$ , we expect the parasites to decay off so that the severity of malaria infection is reduced to near zero or totally eliminated. On the other hand, if  $R_v > 1$ , the malaria infection persists within the human host; that is, more red blood cells and susceptible hepatocytes are infected. This implies that the vaccines may not be efficacious; their use do not eradicate malaria infection among infected individuals. The malaria parasites are therefore likely to persist at the erythrocytic stage in an infected individual and subsequently can be transmitted to other persons in close contact via the mosquito vector.

### 3.5. Critical efficacy of blood stage vaccine

**Definition 1:** Vaccine efficacy is interpreted as the proportionate reduction in malaria disease attack rate within a vaccinated person compared to an unvaccinated person (Small, Cheng, & Ten, 2010).

Generally, the vaccine efficacy  $V_E$  is expressed as follows (Orenstein, Wassilak, Strebel, Bernier, & Blackwelder, 1990):

$$V_E = \frac{ARU - ARV}{ARU} \times 100, \quad (31)$$

where  $ARU$  is the parasite attack rate of unvaccinated individual and  $ARV$  is the attack rate for vaccinated people. A critical vaccine efficacy therefore refers to the minimum efficacy value beyond which the vaccine is capable of eradicating the infection from the human host. To establish a critical malaria vaccine efficacy from the vaccine reproduction number (13), we assume that only the blood stage vaccine is administered to the individual. That is,  $\nu = 0$ ,  $b = 0$ ,  $\chi = 0$ . We then solve for  $\varrho$  from the equation  $R_v = 1$  as follows:

$$\frac{P(1-\pi)(1-a)(1-\varrho)\gamma\beta_r\lambda_r\mu_c}{\left(\frac{(1-\varrho)\tau k_c\lambda_w}{\mu_w} + \mu_c\right)\left(\frac{(1-\varrho)\tau k_t\lambda_w}{\mu_w} + \gamma + \mu_t\right)} = \mu_r \left(\frac{d\tau\lambda_w + \mu_w}{\mu_w}\right)^2 \left(\mu_m + \frac{\beta_r\lambda_r}{\mu_r}\right). \quad (32)$$

By simplification, Equation (32) reduces to

$$\frac{(1-\varrho)\mu_w^2}{(\mu_c\mu_w + (1-\varrho)\tau k_t\lambda_w)(\mu_w(\gamma + \mu_t) + (1-\varrho)\tau k_c\lambda_w)} = \Delta, \quad (33)$$

where

$$\Delta = \frac{\mu_r \left(\frac{d\tau\lambda_w}{\mu_w} + 1\right) (d\tau\lambda_w + \mu_w) \left(\mu_m + \frac{\beta_r\lambda_r}{\mu_r}\right)}{(1-\pi)(1-a)\gamma P\mu_c\beta_r\lambda_r\mu_w}. \quad (34)$$

Upon solving for  $(1-\varrho)$  in (33) using the quadratic formula, we obtain

$$(1-\varrho) = \frac{-\mathcal{B}_1 \pm \sqrt{\mathcal{B}_1^2 - 4(\mathcal{B}_2\mathcal{B}_0)}}{2\mathcal{B}_2}, \quad (35)$$

where

$$\mathcal{B}_0 = -\Delta\mu_c(\gamma + \mu_t)\mu_w^2, \quad \mathcal{B}_1 = -\mu_w(\Delta\tau k_c\lambda_w(\gamma + \mu_c + \mu_t) - \mu_w), \quad \text{and} \\ \mathcal{B}_2 = -\Delta(\tau k_c\lambda_w)^2.$$

From Equation (35), the critical efficacy of the blood stage vaccine,  $0 < \varrho_c < 1$ , is

$$\varrho_c = 1 - \left(\frac{-\mathcal{B}_1 \pm \sqrt{\mathcal{B}_1^2 - 4(\mathcal{B}_2\mathcal{B}_0)}}{2\mathcal{B}_2}\right), \quad (36)$$

where  $\mathcal{B}_i$ ,  $i = \{0, 1, 2\}$ , are as defined in Equation (35).

Equation (36) implies that for any blood stage vaccine to effectively control clinical malaria, then its efficacy must be higher than the stated critical vaccine efficacy.



Differentiating  $R_v$  with respect to vaccine efficacy  $\varrho$  yields

$$\begin{aligned} \frac{\partial R_v}{\partial \varrho} = & -\frac{P(1-\pi)(1-a)\beta_r\lambda_r\mu_c\gamma}{\mu_r\left(\mu_m + \frac{\beta_r\lambda_r}{\mu_r}\right)\left(\frac{(1-e)\tau k_c\lambda_w}{\mu_w} + \mu_c\right)\left(\frac{d\tau\lambda_w}{\mu_w} + 1\right)^2\Psi_3} \\ & + \frac{P(1-\pi)(1-a)\beta_r\lambda_r\mu_c\gamma(1-e)\tau\lambda_w k_t}{\mu_r\mu_w\left(\mu_m + \frac{\beta_r\lambda_r}{\mu_r}\right)\left(\frac{(1-e)\tau k_c\lambda_w}{\mu_w} + \mu_c\right)\left(\frac{d\tau\lambda_w}{\mu_w} + 1\right)^2\Psi_3^2} \\ & + \frac{P(1-\pi)(1-a)\beta_r\lambda_r\mu_c\gamma(1-e)\tau\lambda_w k_c}{\mu_r\mu_w\left(\mu_m + \frac{\beta_r\lambda_r}{\mu_r}\right)\left(\frac{(1-e)\tau k_c\lambda_w}{\mu_w} + \mu_c\right)^2\left(\frac{d\tau\lambda_w}{\mu_w} + 1\right)^2\Psi_3}, \end{aligned} \tag{37}$$

where  $\Psi_3 = (((1-\varrho)\tau k_t\lambda_w)/\mu_w) + \gamma + \mu_t$ .

We further simplify the right-hand side (RHS) of (37) by making the following representations: let  $\Psi_1 = \mu_r(\mu_m + ((\beta_r\lambda_r)/\mu_r))$ ,  $\Psi_2 = (((1-\varrho)\tau k_c\lambda_w)/\mu_w) + \mu_c$  and  $\Psi_4 = (1 + ((d\tau\lambda_w)/\mu_w))$ . This results in

$$\frac{\partial R_v}{\partial \varrho} = \frac{P(1-\pi)(1-a)\beta_r\lambda_r\mu_c\gamma(1-\varrho)\tau\lambda_w k_t k_c}{\Psi_1\Psi_2\Psi_3\Psi_4^2} \left\{ \frac{1}{\mu_w k_c \Psi_3} + \frac{1}{\mu_w k_t \Psi_2^2} - \Gamma \right\}, \tag{38}$$

where  $\Gamma = (1/(1-\varrho)\tau\lambda_w k_c k_t)$ . We observe that  $(\partial R_v/\partial \varrho) < 0$  when  $\mu_c\mu_w^2(\gamma + \mu_t) > \tau k_c k_t \lambda_w^2(1-\varrho)$ .  $R_v$  is therefore a decreasing function of the blood stage vaccine  $\varrho$ . This means that an efficacious BSV reduces the density of IRB cells within the human host. Figure 4 shows the profiles of the density of blood trophozoites and blood schizonts as a function of the efficacy of the BSV,  $\varrho$ . The concentration of infected erythrocytes decreases with increasing values of  $\varrho$ .

## 4. Numerical simulation

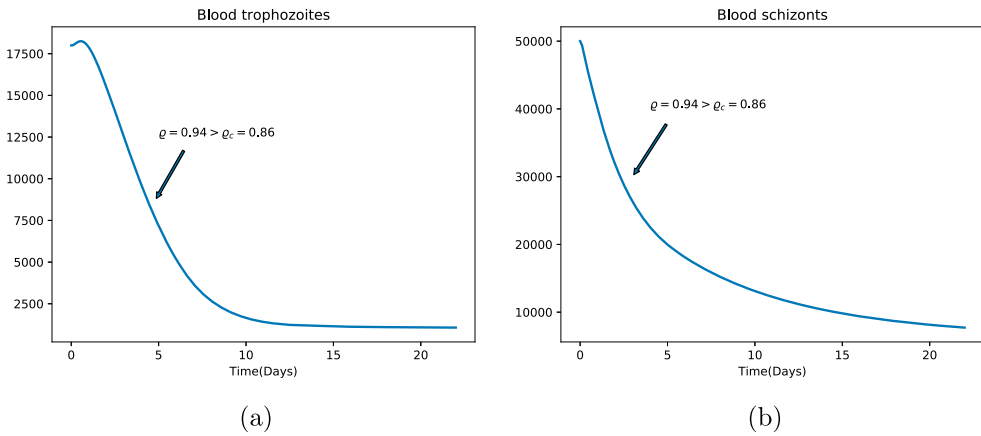
### 4.1. Vaccine efficacy

**Lemma 4.1:** *The vaccination threshold  $R_v < 1$  whenever  $\varrho > \varrho_c$*

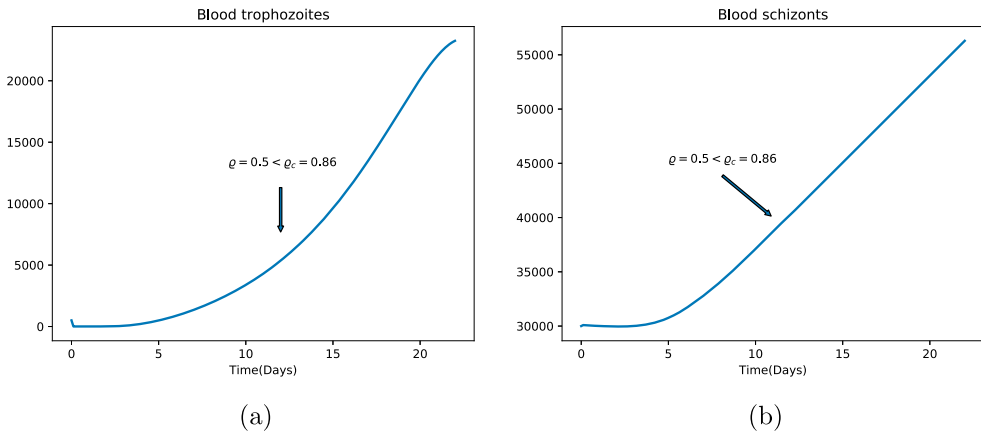
When the efficacy of the BSV is higher than the critical vaccine efficacy  $\varrho_c$ , the merozoites are eradicated from the blood stream. Under this setting, the capacity of the blood stage vaccine to eradicate malaria parasites in the host’s blood stream is guaranteed by Lemma 4.1. The results of Lemma 4.1 is shown numerically in Figure 3(a) and (b) using different values of  $\varrho$ . In Figure 3, a blood stage vaccine with a minimum efficacy of 94% is needed to control the blood stage parasites. Using the provided parameter values and expression (13), we observe that under this condition,  $R_v$  is less than unity. That is  $R_v = 0.58 < 1$ .

**Lemma 4.2:** *The vaccination threshold  $R_v > 1$  whenever  $\varrho < \varrho_c$*

When the efficacy of the blood stage vaccine is lower than the critical efficacy ( $\varrho < \varrho_c$ ), the rate of infection of susceptible infected red blood cells is higher. This leads to increased density of infected red blood cells (blood trophozoites and blood schizonts) as shown in



**Figure 3.** Graphs showing the density of (a) blood trophozoites  $T(t)$  and (b) blood schizonts  $C(t)$  when the blood stage vaccine efficacy,  $\rho = 0.94 > \rho_c = 0.86$  and  $R_v = 0.58 < 1$ . The parameter values are available in Table 4.



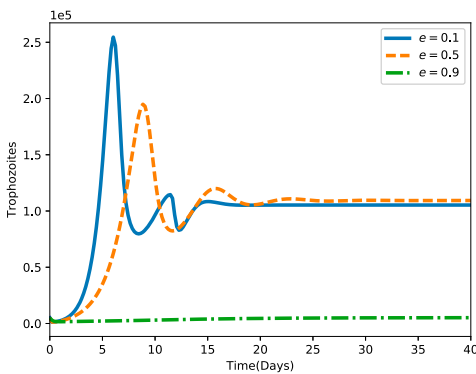
**Figure 4.** Graphs showing the density of (a) blood trophozoites  $T(t)$  and (b) blood schizonts  $C(t)$  when the efficacy of blood stage vaccine,  $\rho = 0.5 < \rho_c = 0.86$  and  $R_v = 1.27 > 1$ . The used parameters values are available in Table 4.

Figure 4. Using the parameter values in Table 4 and the expression for the vaccine reproduction number, we observe that the above condition is only guaranteed when  $R_v$  is greater than unity. That is,  $R_v = 1.27 > 1$ .

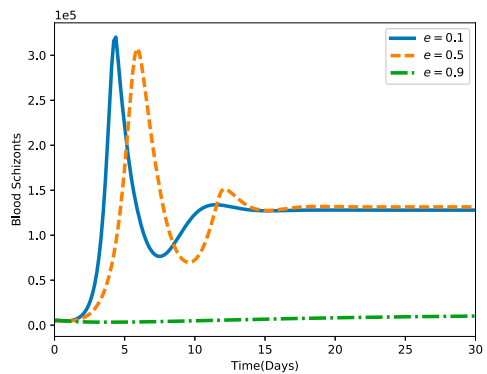
Only a highly efficacious blood stage vaccine, ( $\rho > 90\%$ ) would guarantee the achievement of a malaria free equilibrium as shown in Figure 5. A blood stage vaccine with lower efficacy, ( $\rho < 50\%$ ) is likely to be less effective in clearing the malaria parasites. A malaria persistent steady state is hence probable (see Figure 5). The concentration of gametocytes in the blood stream is indirectly influenced by the blood stage vaccine. Higher vaccine efficacy minimizes the concentration of gametocytes that are later sucked up by feeding anopheles mosquitoes. As the efficacy of blood stage vaccine diminishes, higher concentration of gametocytes is observed in the blood stream as shown in Figure 6.

**Table 4.** Parameter values used in the numerical simulations and sensitivity analysis.

Parameter	Value	Range	Units	Source
$P$	16	(15–20)	/erythrocytes/day	Diebner et al. (2000)
$k_x$	0.01	(0.001–0.9)	/day	Chiyaka et al. (2008)
$k_t$	0.01	(0.001–0.9)	/day	Chiyaka et al. (2008)
$k_c$	0.000001	(0.001–0.9)	/day	Chiyaka et al. (2008)
$\mu_r$	0.083	(0.05–0.1)	/day	Anderson et al. (1989)
$\beta_r$	$2.0 \times 10^{-1}$	(0.07–0.3)	/mm <sup>3</sup> /day	Dondorp, Kager, Vreeken, and White (2000)
$\beta_s$	$1.0 \times 10^{-3}$	(0.001–0.2)	/mm <sup>3</sup> /day	Selemani, Luboobi, and Nkansah-Gyekye (2016)
$\pi$	0.2	(0.1–0.9)	unitless	Talman, Domarle, McKenzie, Arie, and Robert (2004)
$\mu_h$	0.029	(0.01–0.5)	/day	Estimated
$\mu_x$	0.02	(0.01–1)	/day	Selemani et al. (2016)
$\lambda_r$	$3 \times 10^3$	$(3 \times 10^3 - 3 \times 10^8)$	cells/ml/day	Li et al. (2011)
$\lambda_h$	$3 \times 10^5$	$(3 \times 10^5 - 3 \times 10^8)$	cells/ $\mu$ l <sup>-1</sup> /day	Tumwiine, Mugisha, and Luboobi (2008)
$\lambda_w$	30	(10–40)	/ $\mu$ l <sup>-1</sup> /day	Chiyaka, Garira, and Dube (2010)
$\mu_m$	48	(46–50)	/day	Li et al. (2011)
$\Lambda$	30	(18–35)	sporozoites/day	Selemani et al. (2016)
$\mu_s$	1.2	(1.0 – 2.4)	/day	Selemani et al. (2016)
$\mu_t$	0.5	(0.01–0.8)	/day	Magombedze et al. (2011)
$\mu_c$	0.5	(0.01–0.9)	/day	Magombedze et al. (2011)
$\mu_g$	0.0000625	$(6.0 \times 10^{-5} - 7.0 \times 10^{-5})$	/day	Selemani et al. (2016)
$\mu_w$	2	(0.05–3)	/day	Chiyaka et al. (2010)
$\delta_x$	1e-5	(1e-5–1e-7)	mm <sup>-3</sup> /day	Chiyaka et al. (2010)
$\delta_t$	0.05	(0.01–0.08)	mm <sup>-3</sup> /day	Chiyaka et al. (2010)
$\delta_c$	0.05	(0.01–0.08)	mm <sup>-3</sup> /day	Chiyaka et al. (2010)
$\gamma$	1.5	(0.1–2)	/day	Selemani et al. (2016)
$\chi$	0.2	(0–1)	unitless	Assumed
$\rho$	0.45	(0–1)	unitless	Birkett (2016)
$\nu$	0.3	(0–1)	unitless	Assumed
$\tau$	1.5	(1–2)	unitless	Niger and Gumel (2011)
$b$	0.2	(0–1)	unitless	Niger and Gumel (2011)
$a$	0.2	(0–1)	unitless	Niger and Gumel (2011)
$d$	0.0005	(0.00005–0.02)	unitless	Magombedze et al. (2011)
$N$	10,000	(8000–20,000)	/day	Tumwiine et al. (2014)



(a)



(b)

**Figure 5.** Simulations showing the effect varying the parameter  $\rho$  on the density of infected red blood cells. All other parameter values are in Table 4.

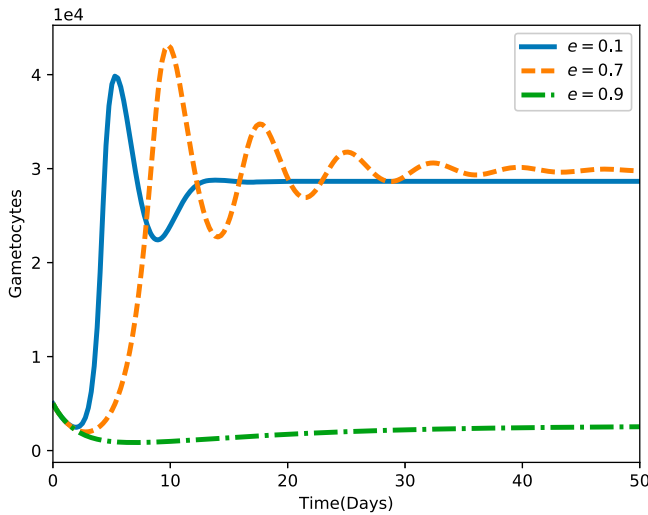


**Figure 6.** Simulations showing the effect varying the parameter  $\rho$  on the concentration of gametocytes in blood. All other parameter values are in Table 4.

The effect of BSV-induced reduction of merozoites released per bursting blood schizont is monitored by differentiating  $R_v$  with respect to  $a$ . This gives

$$\frac{\partial R_v}{\partial a} = - \frac{(1 - \pi)\gamma(1 - \rho)P\mu_c\beta_r\lambda_r}{\mu_r \left( \mu_m + \frac{\beta_r\lambda_r}{\mu_r} \right) \left( 1 + \frac{d\tau\lambda_w}{\mu_w} \right)^2 \left( \frac{(1-\rho)\tau k_c\lambda_w}{\mu_w} + \mu_c \right) \Psi_3} < 0,$$

where  $\Psi_3 = (((1 - \rho)\tau k_t\lambda_w)/\mu_w) + \gamma + \mu_t$ .

We make the following observations: the vaccine reproduction number  $R_v$  decreases with increasing value of  $a$ . As less blood schizonts burst, less merozoites are released and hence less secondary infections that increase the severity of the disease as displayed in Figure 7. This leads to the reduction in the vaccine reproduction number and hence the density of infected red blood cells in the blood stream.

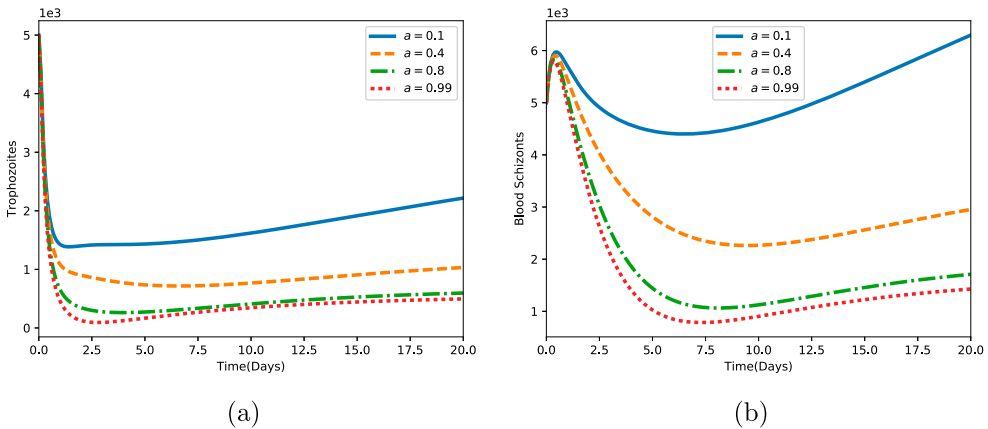


**Figure 7.** Simulations showing the effect varying the parameter  $a$  on the density of (a) blood trophozoites  $T(t)$  and (b) blood schizonts  $C(t)$ . All other parameter values are in Table 4.

The effect of the BSV-induced enhanced production of CD8+ T cells is monitored by the partial derivatives of  $R_v$  with respect to  $\tau$ .

$$\frac{\partial R_v}{\partial \tau} = -\frac{(1-\pi)(1-a)\gamma(1-e)^2 P k_c \mu_c \beta_r \lambda_r \lambda_w}{\mu_r \mu_w \left(\frac{d\tau \lambda_w}{\mu_w} + 1\right)^2 \left(\mu_m + \frac{\beta_r \lambda_r}{\mu_r}\right) \left(\frac{(1-e)\tau k_c \lambda_w}{\mu_w} + \mu_c\right)^2 \Psi_3} - \frac{(1-\pi)(1-a)\gamma(1-e)^2 P k_t \mu_c \beta_r \lambda_r \lambda_w}{\mu_r \mu_w \left(\frac{d\tau \lambda_w}{\mu_w} + 1\right)^2 \left(\mu_m + \frac{\beta_r \lambda_r}{\mu_r}\right) \left(\frac{(1-e)\tau k_c \lambda_w}{\mu_w} + \mu_c\right)^2 \Psi_3^2} - \frac{2(1-\pi)(1-a)\gamma d(1-e) P \mu_c \beta_r \lambda_r \lambda_w}{\mu_r \mu_w \left(\frac{d\tau \lambda_w}{\mu_w} + 1\right)^3 \left(\mu_m + \frac{\beta_r \lambda_r}{\mu_r}\right) \left(\frac{(1-e)\tau k_c \lambda_w}{\mu_w} + \mu_c\right)^2 \Psi_3}, \tag{39}$$

where  $\Psi_3 = (((1-\varrho)\tau k_t \lambda_w)/\mu_w) + \gamma + \mu_t$ .

By applying the algebraic substitutions used in Equations (38) and (39) simplifies to

$$\frac{\partial R_v}{\partial \tau} = -\frac{\Theta^*}{\Psi_1 \Psi_2 \Psi_3 \Psi_4^2} \left( \frac{1}{dk_t \Psi_2} + \frac{1}{dk_c \Psi_3} + \frac{2}{(1-e)k_c k_t \Psi_4} \right) < 0, \tag{40}$$

where

$$\Theta^* = (1-\pi)(1-a)\gamma P(1-e)^2 dk_c k_t \mu_c \beta_r \lambda_r \lambda_w.$$

We observe from (40) that  $R_v$  decreases with increasing  $\tau$ . As more CD8+ T cells are activated, more trophozoites and blood schizonts are killed through phagocytosis, leading to reduction in the severity of malaria infection as shown in Figure 8.

The effect of the BSV-induced reduction in the burst size  $P$  of infected red blood cells is shown by the following formula:

$$\frac{\partial R_v}{\partial P} = \frac{(1-\pi)(1-a)\gamma(1-e)\mu_c \beta_r \lambda_r \mu_c}{\mu_r \left(\frac{d\tau \lambda_w}{\mu_w} + 1\right) (d\tau \lambda_w + \mu_w) \left(\mu_m + \frac{\beta_r \lambda_r}{\mu_r}\right) \left(\frac{(1-e)\tau k_c \lambda_w}{\mu_w} + \mu_c\right)^2 \Psi_3},$$

where  $\Psi_3 = (((1-\varrho)\tau k_t \lambda_w)/\mu_w) + \gamma + \mu_t$ .

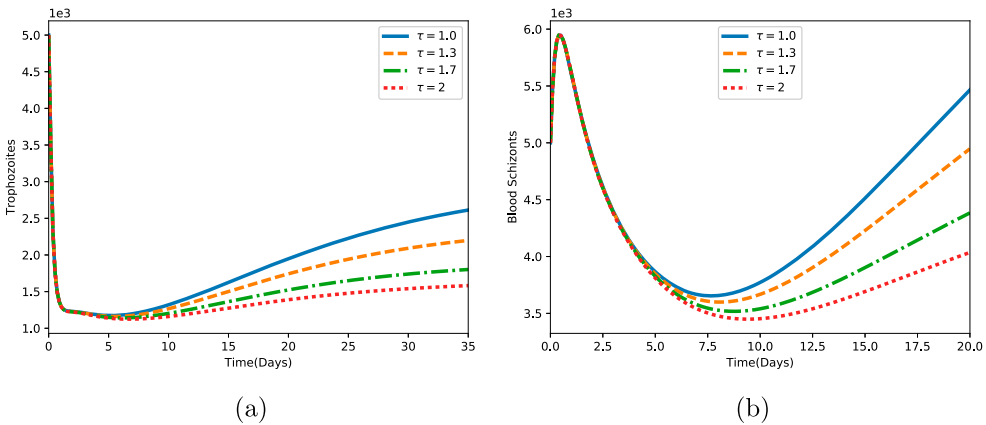


**Figure 8.** Simulation showing the density of (a) blood trophozoites  $T(t)$  and (b) blood schizonts  $C(t)$  for varying values of blood stage vaccine-induced enhanced production parameter  $\tau$ . All other parameter values are in Table 4.

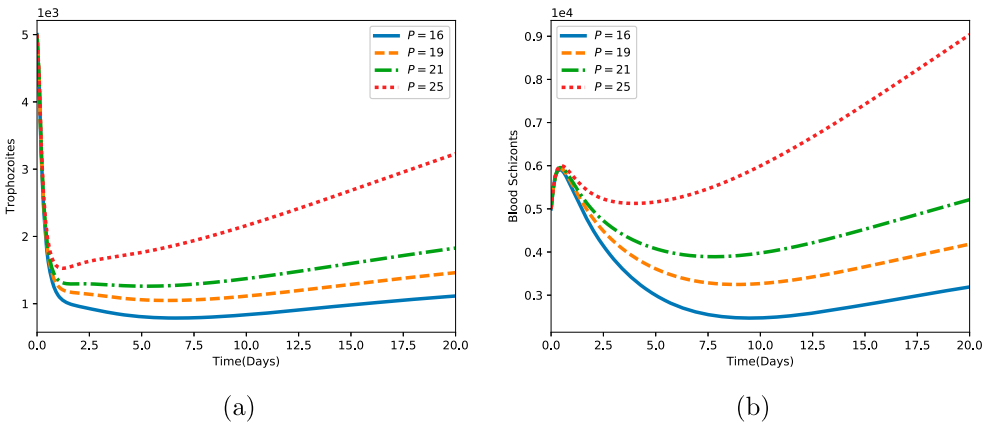


**Figure 9.** Simulations showing how the infected red blood cell burst size  $P$  affects the density of (a) blood trophozoites  $T(t)$  and (b) blood schizonts  $C(t)$ . All other parameter values are in Table 4.

Note that  $(\partial R_v / \partial P) > 0$  and  $R_v$  decreases (increases) with decreasing (increasing) value of  $P$ . The higher the density of released merozoites from bursting blood schizonts, the higher the rate of secondary invasions at the blood stage. The concentration of infected red blood cells in blood is observed to increase with increasing value of  $P$  as shown in Figure 9. An efficacious malaria vaccine would be necessary in minimizing secondary and future invasions that occur at the blood stage of malaria infection.

#### 4.2. Threshold analysis and vaccine impacts

The Malaria Vaccine Technology Road map updated in November 2013 has two key strategic goals targeting *P. falciparum* and *P. vivax* malaria by the year 2030: (1) to develop vaccines with over 75% protective efficacy against clinical malaria and (2) to develop transmission blocking vaccines thereby reducing new cases of human malaria infections (MVFG, 2018). A combination of malaria vaccines (pre-erythrocytic, blood stage

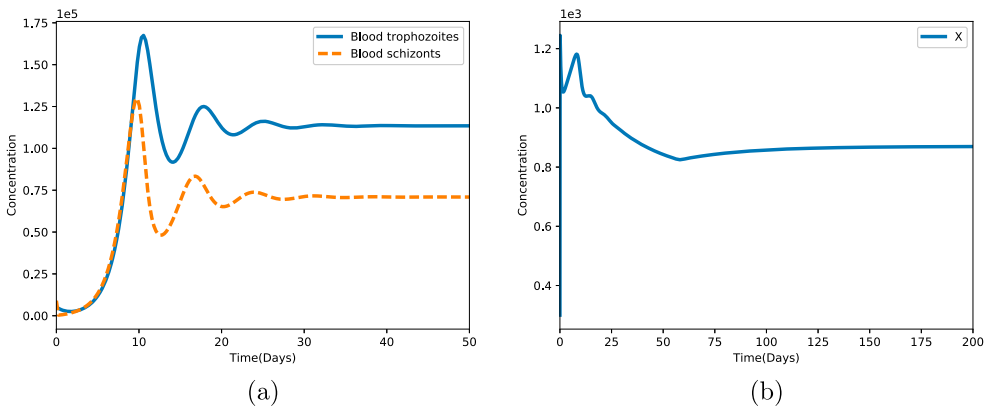


**Figure 10.** Time profile of the total concentration of infected red blood cells (a) and the concentration of infected liver hepatocytes (b) in the absence of malaria vaccines ( $\varrho = \chi = \nu = 0$ ). All parameter values are in Table 4.

and transmission blocking vaccines) could help in achieving the over 75% strategic goal (Miura, 2016).

A highly efficacious blood stage vaccine has a potential to significantly reduce the numbers of gametocytes in the blood stream, thereby minimizing parasite transmission to mosquitoes and subsequently to other human beings. In the following section, we investigate the possible impacts of different malaria vaccine combinations with varying degrees of efficacy.

In the absence of malaria vaccines,  $\varrho = \chi = \nu = 0$ , we observe from Figure 13 that the concentration of infected red blood cells increases rapidly and settles at the parasite persistent equilibrium point. This trend is also observed with the infected liver hepatocytes (see Figure 10b). The concentration of infected liver hepatocytes rises due to invasion by

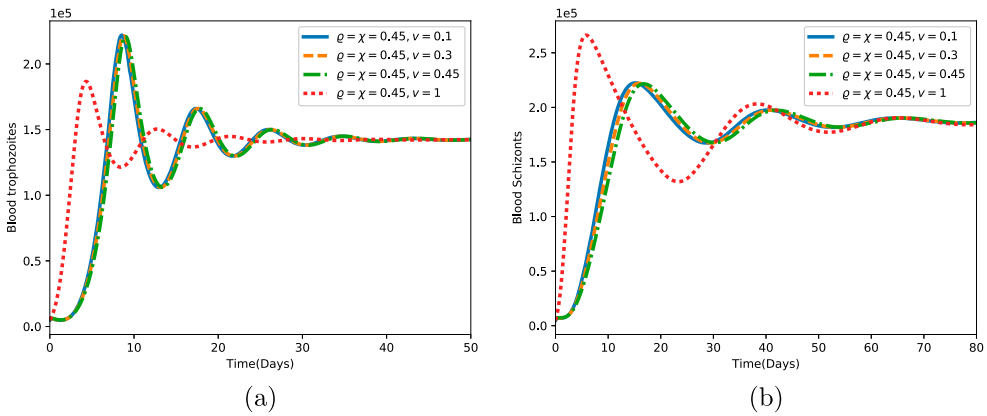


**Figure 11.** Time profile of the total concentration of (a) blood trophozoites and blood schizonts (b) for  $\varrho = \chi = 0.45$  with varying efficacy of pre-erythrocytic vaccine  $\nu$ . The set of parameter values is given in Table 4.

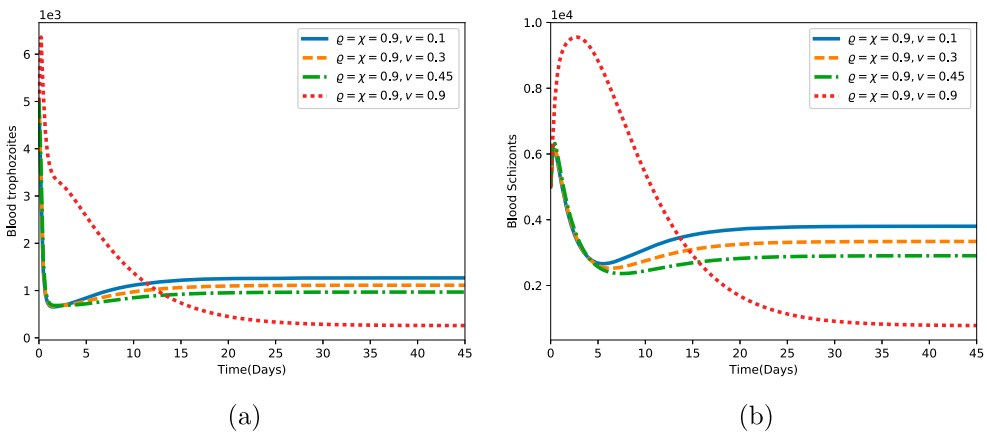


**Figure 12.** Time profile of the total concentration of (a) blood trophozoites and blood schizonts (b) for  $\varrho = \chi = 0.9$  with varying efficacy of pre-erythrocytic vaccine  $\nu$ . The set of parameter values is given in Table 4.

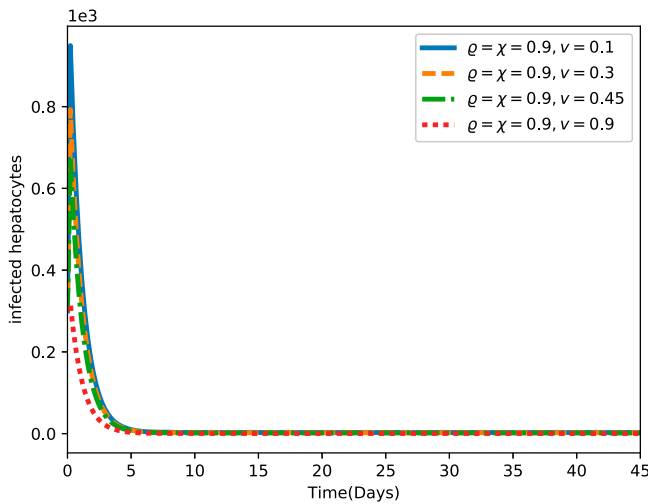


**Figure 13.** Simulation showing the profile of infected liver hepatocytes in the presence of perfect malaria vaccines ( $\varrho = \chi = 0.9$ ). The efficacy of the pre-erythrocytic vaccine  $\nu$  is varied from 0 to 1. The set of parameter values is given in Table 4.

sporozoites for about a week. This is followed by a slight decline in density and subsequent persistent concentration at the liver stage.

A malaria vaccine with an efficacy of 45% may not be adequate in eliciting sufficient immune response to reduce and clear infections as shown in Figure 11. More plasmodium parasites are likely to persist in the blood stream, raising the severity of infections.

A combination of an imperfect blood stage vaccine (efficiency  $\geq 90\%$ ) and an imperfect transmission blocking vaccine (efficiency  $\geq 90\%$ ) is likely to result in rapid eradication of the infected infected red blood from the human host as displayed in Figure 12. Observe that the parasite free equilibrium is highly probable irrespective of the efficacy of the pre-erythrocytic vaccine in this context.

Similarly, the concentration of gametocytes in the blood stream is observed to diminish quickly in the presence of efficacious malaria vaccine combinations (see Figure 13).

## 5. Discussion

Using numerical simulation, we observe that the activated CD8+ T cells and malaria vaccines have a considerable effects on malaria control. Vaccination reduces the basic reproduction number by a constant factor. An imperfect blood stage vaccine with an efficacy of at least 90% is shown to be very effective in controlling in-host *P. falciparum* malaria.

We further observe that malaria vaccines that minimize the total number of merozoites released per bursting infected liver hepatocytes, reduce the concentrations of blood trophozoites and blood schizonts. Similarly, a highly efficacious vaccine greatly reduces the burst size of the blood schizonts, so that less merozoites are released from the infected red blood cells. This has the potential to reduce malaria severity and hence malaria transmission to the mosquito vector.



An efficacious blood stage vaccine should maximize the rate of activation of CD8+ T cells. We notice that the higher the vaccine potential to activate these immune cells, the lower the concentration of infected red blood cells in the host.

Our analysis further shows that different vaccine combinations yield different results. In the absence of vaccine therapy, the concentration of infected red blood cells (blood trophozoites and blood schizonts) is shown to increase and stabilize at the parasite persistent equilibrium. An imperfect pre-erythrocytic vaccine with an efficacy of at least 90% is also shown to guarantee the attainment of a parasite free equilibrium.

Like many other epidemic models, the presented in-host malaria model is formulated based on several model assumptions. The parameter values used in the study are also obtained from past literature. The results of our study should therefore be approached with some discretion. The presented model ignores the biology of CD8+ T activation and assumes constant parameter values. It would therefore be difficult to predict with higher accuracy, the optimal malaria vaccine efficacy. In spite of the stated shortcomings, the presented in-host malaria model provides useful insights on the need to improve the efficacy of current malaria vaccines in development and the need to try vaccine combinations in controlling clinical *P. falciparum* malaria infection.

Although the normalized forward sensitivity approach is helpful in identifying important parameters in the dynamics of the disease, it fails to explain the considerable uncertainties in estimating parameter values and hence parameter influences on specific output variables/states in the model. For future improvement of the above model, we recommend the inclusion uncertainty and sensitivity analysis with respect to infected cells of the in-host malaria model based on Latin Hypercube Sampling and Partial Rank Correlation Coefficient.

## 6. Conclusion

We have presented a mathematical model for in-host malaria dynamics subject to malaria vaccines. The analysed model provides useful insights in individual and combined vaccine impacts in reducing the severity of clinical malaria. The notion of critical vaccine efficacy is key in the development of malaria vaccines with the potential to eliminate or eradicate *P. falciparum* malaria in individuals infected with the disease.

In order to achieve a substantial reduction in malaria mortality and morbidity, the efficacy of the malaria vaccine should be higher than the corresponding critical vaccine efficacy. For instance, when the efficacy of the blood stage vaccine is lower than the critical efficacy ( $\varrho < \varrho_c$ ), the rate of infection of susceptible infected red blood cells is higher and clinical malaria persists. However, the concentration of blood trophozoites and blood schizonts decreases drastically if the efficacy of the blood stage vaccine is higher than the critical blood stage vaccine efficacy.

The combined administration of malaria vaccines (Miura, 2016) and antimalarial drugs is likely to provide the much needed therapeutic control against *P. falciparum* malaria. The general and specific impacts generated by vaccine–WHO–antimalarial drugs combination will also form part of our future investigation.

## Disclosure statement

No potential conflicts of interest are disclosed by the authors.

## Funding

The authors acknowledge with gratitude the support from the Institute of Mathematical Sciences, Strathmore University, the National Research Fund (NRF) [NRF- Phd Grant Titus O.O.] Kenya and the DAAD [ST32 - PKZ: 91711149] in the production of this manuscript.

## ORCID

Titus Okello Orwa  <http://orcid.org/0000-0002-0849-1663>

Rachel Waema Mbogo  <http://orcid.org/0000-0003-1639-1360>

Livingstone Serwadda Luboobi  <http://orcid.org/0000-0002-8256-8593>

## References

- Abdulla, S., Oberholzer, R., Juma, O., Kubhoja, S., Machera, F., Membi, C., & Tanner, M.P.H. (2008). Safety and immunogenicity of RTS, S/AS02D malaria vaccine in infants. *New England Journal of Medicine*, 359(24), 2533–2544.
- Agur, Z., Abiri, D., Van der Ploeg (1989). Ordered appearance of antigenic variants of African trypanosomes explained in a mathematical model based on a stochastic switch process and immune-selection against putative switch intermediates. *Proceedings of the National Academy of Sciences*, 86(23), 9626–9630.
- Alonso, P. L., Sacarlal, J., Aponte, J. J., Leach, A., Macete, E., Milman, J., & Cohen, J. (2004). Efficacy of the RTS, S/AS02A vaccine against *Plasmodium falciparum* infection and disease in young African children: Randomised controlled trial. *The Lancet*, 364(9443), 1411–1420.
- Alout, H., Labbé, P., Chandre, F., & Cohuet, A. (2017a). Malaria vector control still matters despite insecticide resistance. *Trends in Parasitology*, 33(8), 610–618.
- Alout, H., Roche, B., Dabiré, R. K., & Cohuet, A. (2017b). Consequences of insecticide resistance on malaria transmission. *PLoS Pathogens*, 13(9), e1006499.
- Anderson, R., May, R., & Gupta, S. (1989). Non-linear phenomena in host-parasite interactions. *Parasitology*, 99(S1), S59–S79.
- Antia, R., Levin, B. R., & May, R. M. (1994). Within-host population dynamics and the evolution and maintenance of microparasite virulence. *The American Naturalist*, 144(3), 457–472.
- Arama, C., & Troye-Blomberg, M. (2014). The path of malaria vaccine development: Challenges and perspectives. *Journal of Internal Medicine*, 275(5), 456–466.
- Arevalo-Herrera, M., Solarte, Y., Yasnot, M. F., Castellanos, A., Rincon, A., Saul, A., & Herrera, S. (2005). Induction of transmission-blocking immunity in Aotus monkeys by vaccination with a *Plasmodium vivax* clinical grade pvs25 recombinant protein. *The American Journal of Tropical Medicine and Hygiene*, 73(5-suppl), 32–37.
- Arriola, Leon M., & Hyman, James M. (2007). Being sensitive to uncertainty. *Computing in Science & Engineering*, 9(2), 10–20.
- Audran, R., Cachat, M., Lurati, F., Soe, S., Leroy, O., Corradin, G., & Spertini, F. (2005). Phase I malaria vaccine trial with a long synthetic peptide derived from the merozoite surface protein 3 antigen. *Infection and Immunity*, 73(12), 8017–8026.
- Austin, D., White, N., & Anderson, R. (1998). The dynamics of drug action on the within-host population growth of infectious agents: Melding pharmacokinetics with pathogen population dynamics. *Journal of Theoretical Biology*, 194(3), 313–339.
- Bertolino, P., & Bowen, D. G. (2015). Malaria and the liver: Immunological hide-and-seek or subversion of immunity from within? *Frontiers in Microbiology*, 6, 41.
- Bhatt, S., Weiss, D., Cameron, E., Bisanzio, D., Mappin, B., Dalrymple, U., & Wenger, E.A. (2015). The effect of malaria control on *Plasmodium falciparum* in Africa between 2000 and 2015. *Nature*, 526(7572), 207.
- Birkett, A. J. (2016). Status of vaccine research and development of vaccines for malaria. *Vaccine*, 34(26), 2915–2920.

- Birkett, A. J., Moorthy, V. S., Loucq, C., Chitnis, C. E., & Kaslow, D. C. (2013). Malaria vaccine R&D in the decade of vaccines: Breakthroughs, challenges and opportunities. *Vaccine*, 31, B233–B243.
- Bojang, K. A., Milligan, P. J., Pinder, M., Vigneron, L., Allouche, A., Kester, K. E., & Yamuah, L. (2001). Efficacy of RTS, S/AS02 malaria vaccine against *Plasmodium falciparum* infection in semi-immune adult men in the gambia: A randomised trial. *The Lancet*, 358(9297), 1927–1934.
- Cai, L., Tuncer, N., & Martcheva, M. (2017). How does within-host dynamics affect population-level dynamics? Insights from an immuno-epidemiological model of malaria. *Mathematical Methods in the Applied Sciences*, 40(18), 6424–6450.
- Carter, R., Mendis, K. N., Miller, L. H., Molineaux, L., & Saul, A. (2000). Malaria transmission-blocking vaccines how can their development be supported? *Nature Medicine*, 6(3), 241.
- Chiyaka, C., Garira, W., & Dube, S. (2008). Modelling immune response and drug therapy in human malaria infection. *Computational and Mathematical Methods in Medicine*, 9(2), 143–163.
- Chiyaka, C., Garira, W., & Dube, S. (2010). Using mathematics to understand malaria infection during erythrocytic stages.
- Derbyshire, E. R., Mota, M. M., & Clardy, J. (2011). The next opportunity in anti-malaria drug discovery: The liver stage. *PLoS Pathogens*, 7(9), e1002178.
- Diebner, H. H., Eichner, M., Molineaux, L., Collins, W. E., Jeffery, G. M., & Dietz, K. (2000). Modelling the transition of asexual blood stages of *Plasmodium falciparum* to gametocytes. *Journal of Theoretical Biology*, 202(2), 113–127.
- Diekmann, O., Heesterbeek, J. A. P., & Metz, J. A. (1990). On the definition and the computation of the basic reproduction ratio  $r_0$  in models for infectious diseases in heterogeneous populations. *Journal of Mathematical Biology*, 28(4), 365–382.
- Dondorp, A. M., Kager, P. A., Vreeken, J., & White, N. J. (2000). Abnormal blood flow and red blood cell deformability in severe malaria. *Parasitology Today*, 16(6), 228–232.
- Dondorp, A. M., Yeung, S., White, L., Nguon, C., Day, N. P., Socheat, D., & Von Seidlein, L. (2010). Artemisinin resistance: Current status and scenarios for containment. *Nature Reviews Microbiology*, 8(4), 272.
- Duffy, P. E., Sahu, T., Akue, A., Milman, N., & Anderson, C. (2012). Pre-erythrocytic malaria vaccines: Identifying the targets. *Expert Review of Vaccines*, 11(10), 1261–1280.
- Greenwood, B., & Targett, G. (2009). Do we still need a malaria vaccine? *Parasite Immunology*, 31(9), 582–586.
- Haldar, K., Murphy, S. C., Milner Jr, D. A., & Taylor, T. E. (2007). Malaria: Mechanisms of erythrocytic infection and pathological correlates of severe disease. *Annual Review of Pathology: Mechanisms of Disease*, 2, 217–249.
- Heesterbeek, J., & Dietz, K. (1996). The concept of  $r_0$  in epidemic theory. *Statistica Neerlandica*, 50(1), 89–110.
- Hellriegel, B. (1992). Modelling the immune response to malaria with ecological concepts: Short-term behaviour against long-term equilibrium. *Proceedings of the Royal Society of London B*, 250(1329), 249–256.
- Hetzel, C., & Anderson, R. (1996). The within-host cellular dynamics of bloodstage malaria: Theoretical and experimental studies. *Parasitology*, 113(1), 25–38.
- Hisaeda, H., Stowers, A. W., Tsuboi, T., Collins, W. E., Sattabongkot, J. S., Suwanabun, N., & Kaslow, D. C. (2000). Antibodies to malaria vaccine candidates pvs25 and pvs28 completely block the ability of *Plasmodium vivax* to infect mosquitoes. *Infection and Immunity*, 68(12), 6618–6623.
- Homan, T. (2016). *Impact of odour-baited mosquito traps for malaria control* (PhD thesis). Wageningen University.
- Ishino, T., Yano, K., Chinzei, Y., & Yuda, M. (2004). Cell-passage activity is required for the malarial parasite to cross the liver sinusoidal cell layer. *PLoS Biology*, 2(1), e4.
- Kamangira, B., Nyamugure, P., & Magombedze, G. (2014). A theoretical mathematical assessment of the effectiveness of coartemether in the treatment of *Plasmodium falciparum* malaria infection. *Mathematical Biosciences*, 256, 28–41.
- Li, Y., Ruan, S., & Xiao, D. (2011). The within-host dynamics of malaria infection with immune response. *Mathematical Biosciences and Engineering*, 8(4), 999–1018.

- Liehl, P., Meireles, P., Albuquerque, I. S., Pinkevych, M., Baptista, F., Mota, M. M., & Prudêncio, M. (2015). Innate immunity induced by plasmodium liver infection inhibits malaria reinfections. *Infection and Immunity*, IAI 02796 IAI-02796 .
- Magombedze, G., Chiyaka, C., & Mukandavire, Z. (2011). Optimal control of malaria chemotherapy. *Nonlinear Analysis: Modelling and Control*, 16(4), 415–434.
- Malaguarnera, L., & Musumeci, S. (2002). The immune response to *Plasmodium falciparum* malaria. *The Lancet Infectious Diseases*, 2(8), 472–478.
- malERA Consultative Group on Vaccines et al. (2011). A research agenda for malaria eradication: Vaccines. *PLoS Medicine*, 8(1), e1000398.
- March, S., Ng, S., Velmurugan, S., Galstian, A., Shan, J., Logan, D. J., & Hoffman, S. L. (2013). A microscale human liver platform that supports the hepatic stages of *Plasmodium falciparum* and *vivax*. *Cell Host & Microbe*, 14(1), 104–115.
- Maude, R. J., Pontavornpinyo, W., Saralamba, S., Aguas, R., Yeung, S., Dondorp, A. M., & White, L. J. (2009). The last man standing is the most resistant: Eliminating artemisinin-resistant malaria in Cambodia. *Malaria Journal*, 8(1), 31.
- Mellouk, S., Berbiguier, N., Druilhe, P., Sedegah, M., Galey, B., Yuan, L., & Hoffman, S. (1990). Evaluation of an in vitro assay aimed at measuring protective antibodies against sporozoites. *Bulletin of the World Health Organization*, 68(Suppl), 52.
- Mellouk, S., Maheshwari, R. K., Rhodes-Feuillette, A., Beaudoin, R. L., Berbiguier, N., Matile, H., & Chigot, J. P. (1987). Inhibitory activity of interferons and interleukin 1 on the development of *Plasmodium falciparum* in human hepatocyte cultures. *The Journal of Immunology*, 139(12), 4192–4195.
- Mikucki, M. A. (2012). *Sensitivity analysis of the basic reproduction number and other quantities for infectious disease models* (PhD thesis). Colorado State University. Libraries.
- Miura, K. (2016). Progress and prospects for blood-stage malaria vaccines. *Expert Review of Vaccines*, 15(6), 765–781.
- Moorthy, V. S., Good, M. F., & Hill, A. V. (2004). Malaria vaccine developments. *The Lancet*, 363(9403), 150–156.
- Mota, M. M., Pradel, G., Vanderberg, J. P., Hafalla, J. C., Frevert, U., Nussenzweig, R. S., & Nussenzweig, V. (2001). Migration of plasmodium sporozoites through cells before infection. *Science*, 291(5501), 141–144.
- MVFG (2018). Malaria vaccine technology roadmap. Autoimmunity Research Foundation. Accessed 14/4/2018 from [http://www.who.int/immunization/topics/malaria/vaccine\\_roadmap/en/](http://www.who.int/immunization/topics/malaria/vaccine_roadmap/en/).
- MVI (2018). Accelerating malaria vaccine development. Accessed 22/2/2018 from <http://www.malariavaccine.org/malaria-and-vaccines/need-vaccine>.
- Nannyonga, B., Mwangi, G., Haario, H., Mbalawata, I. S., & Heilio, M. (2014). Determining parameter distribution in within-host severe *P. falciparum* malaria. *Bio Systems*, 126, 76–84.
- Negal, D., Alemu, A., & Tasew, G. (2016). Malaria vaccine development: Recent advances alongside the barriers. *Journal of Bacteriology and Parasitology*, 7(6).
- Nganou-Makamdop, K., van Gemert, G.-J., Arens, T., Hermsen, C. C., & R. W. Sauerwein (2012). Long term protection after immunization with *P. berghei* sporozoites correlates with sustained IFN $\gamma$  responses of hepatic CD8+ memory T cells. *PLoS One*, 7(5), e36508.
- Niger, A. M., & Gumel, A. B. (2011). Immune response and imperfect vaccine in malaria dynamics. *Mathematical Population Studies*, 18(2), 55–86.
- Nyabadza, F., Njagarah, J. B., & Smith, R. J. (2013). Modelling the dynamics of crystal meth (tik) abuse in the presence of drug-supply chains in south africa. *Bulletin of Mathematical Biology*, 75(1), 24–48.
- Ogutu, B. R., Apollo, O. J., McKinney, D., Okoth, W., Siangla, J., Dubovsky, F., & Malkin, E. (2009). Blood stage malaria vaccine eliciting high antigen-specific antibody concentrations confers no protection to young children in Western Kenya. *PLoS One*, 4(3), e4708.
- Orenstein, W. A., Wassilak, S. G., Strebel, P. M., Bernier, R. H., & Blackwelder, W. C. (1990). Efficacy of pertussis vaccine. *The Journal of Pediatrics*, 117(3), 508.

- Orwa, T. O., Mbogo, R. W., & Luboobi, L. S. (2018). Mathematical model for hepatocytic-erythrocytic dynamics of malaria. *International Journal of Mathematics and Mathematical Sciences*, 2018, Article ID 7019868, 18 pages, 2018. <https://doi.org/10.1155/2018/7019868>.
- Ouattara, A., & Laurens, M. B. (2014). Vaccines against malaria. *Clinical Infectious Diseases*, 60(6), 930–936.
- Pandey, A. K., Reddy, K. S., Sahar, T., Gupta, S., Singh, H., Reddy, E. J., & More, K. R. (2013). Identification of a potent combination of key *Plasmodium falciparum* merozoite antigens that elicit strain-transcending parasite-neutralizing antibodies. *Infection and Immunity*, 81(2), 441–451.
- Pilyugin, S. S., & Antia, R. (2000). Modeling immune responses with handling time. *Bulletin of Mathematical Biology*, 62(5), 869–890.
- Plowe, C. V., Alonso, P., & Hoffman, S. L. (2009). The potential role of vaccines in the elimination of falciparum malaria and the eventual eradication of malaria.
- Polhemus, M. E., Remich, S. A., Ogutu, B. R., Waitumbi, J. N., Otieno, L., Apollo, S., & Ofori-Anyinam, O. (2009). Evaluation of RTS, S/AS02A and RTS, S/AS01B in adults in a high malaria transmission area. *PLoS One*, 4(7), e6465.
- Renia, L., Marussig, M. S., Grillot, D., Pied, S., Corradin, G., Miltgen, F., Del Giudice, G., & Mazier, D. (1991). In vitro activity of CD4+ and CD8+ T lymphocytes from mice immunized with a synthetic malaria peptide. *Proceedings of the National Academy of Sciences*, 88(18), 7963–7967.
- Risco-Castillo, V., Topçu, S., Marinach, C., Manzoni, G., Bigorgne, A. E., Briquet, S., & Silvie, O. (2015). Malaria sporozoites traverse host cells within transient vacuoles. *Cell Host & Microbe*, 18(5), 593–603.
- Rouzine, I. M., & McKenzie, F. E. (2003). Link between immune response and parasite synchronization in malaria. *Proceedings of the National Academy of Sciences*, 100(6), 3473–3478.
- RTS, S. C. T. P. (2011). First results of phase 3 trial of RTS, S/AS01 malaria vaccine in African children. *New England Journal of Medicine*, 365(20), 1863–1875.
- RTS, S. C. T. P. (2012). A phase 3 trial of RTS, S/AS01 malaria vaccine in African infants. *New England Journal of Medicine*, 367(24), 2284–2295.
- Schwenk, R., Asher, L. V., Chalom, I., Lanar, D., Sun, P., White, K., & Krzych, U. (2003). Opsonization by antigen-specific antibodies as a mechanism of protective immunity induced by *Plasmodium falciparum* circumsporozoite protein-based vaccine. *Parasite Immunology*, 25(1), 17–25.
- Seguin, M. C., Klotz, F. W., Schneider, I., Weir, J. P., Goodbary, M., Slayter, M., & Green, S. J. (1994). Induction of nitric oxide synthase protects against malaria in mice exposed to irradiated *Plasmodium berghei* infected mosquitoes: Involvement of interferon gamma and CD8+ T cells. *Journal of Experimental Medicine*, 180(1), 353–358.
- Selemani, M. A., Luboobi, L. S., & Nkansah-Gyekye, Y. (2016). On stability of the in-human host and in-mosquito dynamics of malaria parasite. *Asian Journal of Mathematics and Applications*, 2016, Article ID ama0353, 23 pages ISSN 2307-7743.
- Selemani, M. A., Luboobi, L. S., & Nkansah-Gyekye, Y. (2017). The in-human host and in-mosquito dynamics of malaria parasites with immune responses. *New Trends in Mathematical Sciences*, 5(3), 182–207.
- Sidhu, A. B. S., Verdier-Pinard, D., & Fidock, D. A. (2002). Chloroquine resistance in *Plasmodium falciparum* malaria parasites conferred by pfcrt mutations. *Science*, 298(5591), 210–213.
- Small, D. S., Cheng, J., & Ten Have, T. R. (2010). Evaluating the efficacy of a malaria vaccine. *The International Journal of Biostatistics*, 6(2).
- Soko, W., Chimbari, M. J., & Mukaratirwa, S. (2015). Insecticide resistance in malaria-transmitting mosquitoes in Zimbabwe: A review. *Infectious Diseases of Poverty*, 4(1), 46.
- Sturm, A., Amino, R., Van de Sand, Retzlaff, S., Rennenberg, A., Krueger, A., & V. T. Heussler (2006). Manipulation of host hepatocytes by the malaria parasite for delivery into liver sinusoids. *Science*, 313(5791), 1287–1290.
- Sun, P., Schwenk, R., White, K., Stoute, J. A., Cohen, J., Ballou, W. R., & Krzych, U. (2003). Protective immunity induced with malaria vaccine, RTS, S, is linked to *Plasmodium falciparum* circumsporozoite protein-specific CD4+ and CD8+ T cells producing IFN- $\gamma$ . *The Journal of Immunology*, 171(12), 6961–6967.

- Tabo, Z., Luboobi, L. S., & Ssebuliba, J. (2017). Mathematical modelling of the in-host dynamics of malaria and the effects of treatment. *Journal of Mathematics and Computer Science*, 17(1), 1–21.
- Talman, A. M., Domarle, O., McKenzie, F. E., Arie, F., & Robert, V. (2004). Gametocytogenesis: The puberty of *Plasmodium falciparum*. *Malaria Journal*, 3(1), 24.
- Traoré, B., Sangaré, B., & Traoré, S. (2017). A mathematical model of malaria transmission with structured vector population and seasonality. *Journal of Applied Mathematics*, 2017, Article ID 6754097, 15 pages, 2017. <https://doi.org/10.1155/2017/6754097>
- Tumwiine, J., Hove-Musekwa, S. D., & Nyabadza, F. (2014). A mathematical model for the transmission and spread of drug sensitive and resistant malaria strains within a human population. *ISRN Biomathematics*, 2014, Article ID 636973, 12 pages, 2014. <https://doi.org/10.1155/2014/636973>
- Tumwiine, J., Mugisha, J., & Luboobi, L. (2008). On global stability of the intra-host dynamics of malaria and the immune system. *Journal of Mathematical Analysis and Applications*, 341(2), 855–869.
- Van den Driessche, P., & Watmough, J. (2002). Reproduction numbers and sub-threshold endemic equilibria for compartmental models of disease transmission. *Mathematical Biosciences*, 180(1), 29–48.
- Villarino, N. (2013). CD8+ T cell responses to plasmodium and intracellular parasites. *Current Immunology Reviews*, 9(3), 169–178.
- Wellems, T. E., & Plowe, C. V. (2001). Chloroquine-resistant malaria. *The Journal of Infectious Diseases*, 184(6), 770–776.
- White, M. T., Bejon, P., Olotu, A., Griffin, J. T., Riley, E. M., Kester, K. E., & Ghani, A. C. (2013). The relationship between RTS,S vaccine-induced antibodies, CD4+ T cell responses and protection against *Plasmodium falciparum* infection. *PLoS One*, 8(4), E61395.
- White, N., Pukrittayakamee, S., Hien, T., Faiz, M., Mokuolu, O., & Dondorp, A. (2014). Malaria. *Lancet*, 383, 723–35.
- White, N. J. (2017). Malaria parasite clearance. *Malaria Journal*, 16(1), 88.
- WHO (2015). *World malaria report 2015*. Geneva: World Health Organization.
- WHO (2017a). Malaria fact sheet; 2017. WHO, Geneva. Accessed 22/2/2017 from <http://www.who.int/mediacentre/factsheets/fs094/en/>.
- WHO (2017b). *World malaria report 2017*. Geneva: World Health Organization.